DEVELOPING HEAT TRANSFER FOR LAMINAR FLOW OF POWER-LAW FLUIDS IN THE ENTRANCE REGION OF A PIPE

by

Muhammad Faheem Hassan

A proposal presented to the Faculty of the
American University of Sharjah
College of Engineering
In Partial Fulfillment of
the Requirements
for the Degree of

Master of Science in
Chemical Engineering

Sharjah, United Arab Emirates

June 2022

Declaration of Authorship

I declare that this thesis is my own work and, to the best of my knowledge and belief, it does not contain material published or written by a third party, except where permission has been obtained and/or appropriately cited through full and accurate referencing.

Signed: Muhammad Faheem Hassan

Date: 03-07-2022

Approval Signatures

We, the undersigned, approve the Master's Thesis of Muhammad Faheem Hassan

Thesis Title: DEVELOPING HEAT TRANSFER FOR LAMINAR FLOW OF POWER-LAW FLUIDS IN THE ENTRANCE REGION OF A PIPE

Date of Defense: June 19, 2022

Name, Title, and Affiliation	**Signature**
Dr. Rachid Chebbi Professor, Department of Chemical Engineering Thesis Advisor	
Dr. Zarook Shareefdeen Professor, Department of Chemical Engineering Thesis Committee Member	
Dr. Mehmet Orhan Associate Professor, Department of Mechanical Engineering Thesis Committee Member	
Dr. Sameer Al-Asheh Head Department of Chemical Engineering	
Dr. Lotfi Romdhane Associate Dean College of Engineering	
Dr. Fadi Aloul Dean College of Engineering	
Dr. Mohamed El-Tarhuni Vice Provost for Research and Graduate Studies Office of Research and Graduate Studies	

Acknowledgments

Thanks are due to my advisor Dr. Rachid Chebbi who provided his knowledge, guidance, and insights throughout the research. The work might not be possible without his worthy discussions and constant mentoring.

I am grateful to my committee members Dr. Mohamed Gadalla (late), Dr. Zarook Shareefdeen, and Dr. Mehmet Orhan whose valuable feedback kept me on track and improved the overall quality of the work. I am also thankful to the American University of Sharjah for supporting my studies with the Graduate Teaching Assistantship (GTA), and my professors who taught me courses.

I am especially grateful and indebted to my parents and sisters who always encouraged me to pursue my educational goals and their endless prayers paved the way of my success.

Special thanks are due to my friends Muhammad Ashraf Sabri and Nihal Yasir for believing in me.

Dedication

To my beloved Parents.

Abstract

The objective of this thesis is to develop a model to solve the combined hydrodynamic-thermal entrance region problem for laminar flow of power-law fluids in a circular pipe under uniform wall heat flux condition. The model is based on the inlet-filled region concept of Ishizawa (1966) and uses a boundary layer integral method to solve for the simultaneously developing velocity and thermal profiles. The developed model for power-law fluids uses the hydrodynamic entrance region model developed by Chebbi (2002) for power-law fluids and extends the heat transfer model presented by Al-Ali (1988), and Al-Ali and Selim (1992) for the Newtonian fluid flow case. The axial location at which the thermal boundary layer thickness reaches the circular pipe radius value represents the end of the thermal inlet region. The local Nusselt number asymptotically approaches the fully developed value. The solution is performed in each of the three zones forming the thermal entrance region: hydrodynamic inlet-thermal inlet, hydrodynamic filled-thermal inlet and hydrodynamic filled-thermally filled regions. The local Nusselt number variations along the axial distance of the pipe for power-law indices n = 0.6, 1 and 1.4 and Prandtl number, Pr = 1, 5, 10 and 15 are presented graphically and in tabulated forms. The dimensionless thermal entrance region length is calculated using a Nusselt number criterion (local Nusselt number equal to 1.05 the asymptotic value). Its values at Pr = 5 and for n = 0.6, 1 and 1.4 are 0.3222, 0.3532 and 0.3831, respectively. The Nusselt number asymptotic values for n = 0.6, 1 and 1.4 are 4.49, 4.36 and 4.30, respectively. The present results are in good agreement with the theoretical results in the literature for n=1 (Newtonian fluid case). To my knowledge, no experimental data, numerical or theoretical results asymptotically matching the fully developed solution, are available for the case of simultaneously developing fluid flow and heat transfer for power-law fluid flow in pipes.

Keywords: Non-Newtonian; Power-law; Laminar Flow; Heat Transfer; Hydrodynamic Entrance Region; Thermal Entrance Region; Von Kármán Integral Method.

Table of contents

List of Figures

List of Tables

Glossary of Terms

English letters

A_k	modified kth coefficient of the velocity profile
a_k	k[th] coefficient of the velocity profile
B_k	modified kth coefficient of the thermal profile
b_k	k[th] coefficient of the thermal profile
$\hat{C}_p$	heat capacity per unit mass at constant pressure
D_e	equivalent diameter, m
h	heat transfer coefficient, $kg/(s^3.K)$
k	thermal conductivity of the material
K	consistency index of the power-law fluid
Nu	Nusselt number, hD_e/k
n	power-law fluid index
P	pressure, N/m^2
Pr	Prandtl number, $\mu C_p/k$
P_0	pressure at the entrance, N/m^2
p	$q+2$
q	$1+1/n$
q_0	wall heat flux, w/m^2
R	pipe radius, m
r	radial coordinate in cylindrical coordinates
T	absolute temperature, K
T^*	dimensionless temperature
T_0	fluid entrance temperature, K
T_b	Fluid bulk temperature, K
T_c	centerline temperature, K
T_w	wall temperature, K
U_0	fluid entrance velocity, m/s
U_∞	core velocity, m/s
$\overline{U}_\infty$	dimensionless core velocity
U_c	centerline velocity, m/s

$\bar{U}_c$	dimensionless centerline velocity
$\bar{u}$	dimensionless velocity in x direction
u	velocity component in x direction, m/s
v	velocity component in radial or y direction, m/s
x	a spatial coordinate, axial distance, m
y	distance from the pipe wall, m

Greek Letters

$\bar{\delta}_T$	δ_T/R
Γ_T	thermally filled region shape factor
$\bar{\delta}$	δ/R
δ_T	thermal boundary layer thickness
η_a	apparent viscosity
Γ	hydrodynamic filled region shape factor
α	molecular thermal diffusivity, m^2/s
δ	boundary layer thickness
δ	hydrodynamic boundary layer thickness
η	dimensionless parameter, y/δ y/R or y/δ_T
λ	Pohlhausen's shape factor
μ	dynamic viscosity coefficient, $kg/(m.s)$
ξ	dimensionless axial distance, $x/(R.Re)$
ρ	fluid density kg/m^3
τ	shear stress, $kg/(m.s^2)$

Chapter 1. Introduction

1.1. Non-Newtonian Fluids – Background Information

Fluids, in general, can be categorized into three major classes that is, time independent, time-dependent and visco-elastic. Time-independent fluids may further be grouped as Newtonian, pseudoplastic, dilatant, and Bingham plastic. A mathematical model known as power law model, given in equation (1), has been developed to describe Newtonian, pseudoplastic, and dilatant fluid behaviors.

$$\tau = K\left(\frac{dv}{dy}\right)^{n} \tag{1}$$

For Newtonian fluids, coefficient K is usually denoted by μ which represents fluid viscosity while the flow behavior index n is equal to one. For pseudoplastic fluids n is less than one. Their apparent viscosity decreases with increasing shear rate and thus have a thinning behavior at high shear rate and their apparent viscosity can be written as

$$\eta_a = K\left(\frac{dv}{dy}\right)^{n-1} \tag{2}$$

Here, K is the consistency index, and n is positive and less than one. Polymer solutions, greases, paper pulp, rayon processing, mayonnaise, soaps, detergent slurries, cellulose derivates and their solutions behaves like pseudoplastic fluids.

In contrast to pseudoplastic fluids, dilatant fluids thicken at high shear rates. Equation (2) for apparent viscosity can be used to describe their behavior but with n greater than one. Common fluids of such type are starch suspensions, corn flour solutions and quicksand.

Details and discussion on the mathematical models for Bingham plastic, time-dependent materials and viscoelastic materials are given in [1-4].

1.2. Overview

Fluid flow in circular pipes has many applications. Heat transfer is also important due to its widespread applications in chemical, petrochemical, and food and petroleum processing industries. Three different methods, namely semi-numerical, numerical, and

integral boundary layer methods, are typically employed to solve the thermal entrance region for laminar flow in a pipe. In the first method, first the velocity profile is deducted from the momentum equation through its linearization. Then, the temperature profile can be obtained numerically by employing the obtained velocity profile. In the second method, i.e., the fully numerical velocity and temperature profiles are obtained numerically by solving the momentum and energy equations. In the third method, integral hydrodynamic and thermal boundary using approximate velocity and temperature profiles are used. The solution is obtained using typical boundary layer approximations including: inviscid flow outside the inlet boundary layer region and fluid uninfluenced by heat transfer outside the inlet thermal boundary layer. Many solutions have been proposed in the literature for the case of developing heat transfer assuming fully developed velocity profile. This is definitely a much simpler problem.

The model in [5] divides the entrance region for a laminar power-law fluid flow into two regions: the inlet region in which viscous effects are limited to the boundary layer, and the filled region in which the flow is developing while viscous effects are present in any part of that region. The approach extends the model of Mohanty and Asthana for laminar Newtonian fluid flow in the entrance region of a circular pipe [6].

The thermal entrance region also consists of two regions: the inner region followed by the filled region. The problem is solved successfully for the Newtonian fluid flow case subject to constant wall temperature in [7] using the inlet-filled region concept.

Laminar flow is more common for pseudoplastic fluids as viscosities up to 100 times of the water's viscosity are quite common. Viscosities of liquids are typically a strong function of temperature. The change in viscosity due to temperature effects is needed.

The objective of the present investigation is to solve hydrodynamic-thermal entry length problem for power-law fluids using the inlet-filled region concept along with the von Kármán momentum integral analytical method to solve the momentum and energy equations. Fluid flow is assumed laminar, and the relevant physical properties are assumed constant. Fluid is flowing in a circular pipe, which is subjected to a constant heat flux. Upon extensive literature review, I confidently conclude that there is no recent work done related to the problem under discussion.

The present work accounts for simultaneously developing laminar fluid flow and heat transfer in circular pipes in the case of power-law fluids subjected to constant heat flux. The analysis is used to provide the local Nusselt number needed for the determination of heat transfer coefficients in heat exchangers.

To my knowledge, no experimental data, numerical or theoretical results asymptotically matching the fully developed solution, are available for the case of simultaneously developing fluid flow and heat transfer for power-law fluid flow in pipes. The present theoretical model asymptotically reaches the fully developed solution. Furthermore, the results are validated against published results for the Newtonian fluid flow special case. The model is based on the inlet-filled region concept of Ishizawa [8] and uses the hydrodynamic model in [5] to solve for the simultaneously developing velocity and thermal profiles.

Chapter 2. Literature Review

Fluid flow and heat transfer of power-law fluids in the entrance region of a circular pipe has been investigated extensively. The relevant literature is reviewed below. To the best of the author's knowledge, no previous investigation used the approach proposed in this thesis to solve the problem for power-law fluids.

In 1883, Graetz [9] solved the problem of thermally developing slug flow in a pipe under isothermal conditions. Later in 1885, he solved the problem of parabolic velocity profile. Graetz problem in which heat transfer developments are studied in an isothermal tube is named after him.

1n 1910, Nusselt [10] solved the same problem and presented a non-dimensional heat transfer coefficient known as "Nusselt number". In 1928, Leveque [11] also solved Graetz problem for high Prandtl number fluids. Further details can be found in [12,13].

This problem has been solved by various authors using numerical or analytical techniques [14-17]. Siegel et al. used separation of variables techniques to solve the energy equation to get the solution for the constant wall flux case [18].

Kays solved the simultaneously hydrodynamic-thermal entry length problem in a circular tube [19]. He used an approximate velocity profile while for the energy profile he integrated the energy equation numerically. Hwang [20] and Hwang and Fan [21,22] solved the same problem using numerical methods for flow in channels. Instead of using approximate velocity profile they first solved momentum equation for uniform viscosity fluids and then used this velocity profile to solve energy equation.
The Graetz problem was solved by Lyche and Bird [23] using separation of variables for pseudoplastic fluid flow for the constant wall temperature case.

Yau and Tien [24] solved the simultaneously hydrodynamic-thermal entry length problem for pseudo plastic. They solved it for a rectangular duct using the von Kármán-Pohlhausen integral method to solve the momentum and energy equations.

Mckillop [25] numerically solved the Graetz problem for pseudoplastic fluids in a laminar regime in a circular tube. Two temperature cases were considered i.e., constant wall temperature and constant heat flux. He used an analogous approach to the one used by Goldstein and Atkinson [26] to solve the same problem for Newtonian fluids.

Bird [27] solved the Graetz problem near the entrance using the Lévêque approximation. Chung and Zhang used numerical techniques to determine the Nusselt number of hydrodynamically fully developed and thermally developing laminar flow of pseudoplastic fluids in a rectangular duct entrance region [28]. Since this is a rectangular geometry with both dimensions are of same order of magnitudes therefore, they used finite difference equation with Successive Overrelaxation.

Cotta and Ozisik studied the Graetz problem for laminar flow of non-Newtonian fluid inside a circular tube and a parallel-plate duct subjected to prescribed wall heat flux [29]. They used the separation of variables technique to solve this problem while the sign count method has been used to accurately determine eigenvalues and Eigen functions. When the temperature profile becomes fully developed, then the profile doesn't change in the z-direction anymore. The authors compared result with other results presented in literature and the comparison is given in Table 1 in [29]. He compared it with Bird asymptotic values.

Chaves et al. considered both right angularly and isosceles triangular ducts subjected to constant wall temperature as thermal boundary condition. They used a hybrid analytical-numerical approach based on the generalized integral transform technique (GIIT) to simulate the laminar forced convection for hydrodynamically fully developed and thermally developing laminar flow of power-law fluids inside ducts with a triangular geometry [30]. The authors compared the results for the Newtonian case (n=1) with the literature given results.

Quaresma and Macedo [31] used integral transform technique to analytically solve the thermal entry region in laminar forced convection of Herschel-Bulkley fluids for both circular and parallel-plates ducts, which are maintained at a prescribed wall temperature or at a prescribed wall heat flux. They obtained local Nusselt numbers with high accuracy in both developing and fully developed thermal regions, and also performed the critical comparisons with previously reported numerical results [31].

Quaresma and Lima used analytical method to study the heat transfer in turbulent forced convection of pseudoplastic fluids where flow is thermally developing within a circular tube [32]. Authors solved the equations using splitting up procedure in combination with sign-count method for numerical solution of the associated eigenvalue problem,

and obtain the temperature distributions and consequently, the local Nusselt numbers along the thermal entry and fully developed regions, for different Reynolds and Prandtl numbers and power-law indices. The tube is subjected to a prescribed wall heat flux. But since the authors considered turbulent flow and we are considering laminar flow, so this study doesn't overlap to ours much.

Magno et al. [33] applied the generalized integral transform technique (GITT) to the solution of the boundary layer equations in simultaneously developing laminar flow of both pseudoplastic and dilatant fluids. A stream-function formulation is employed which offers a better computational performance than the primitive variables formulation. Numerical results for the bulk temperature and Nusselt numbers are established at different axial positions along the channel and for various power-law indices. Comparisons with previously reported works in the literature are also performed.

Llorens and Galanic [34] solved the hydrodynamic entrance region problem for power-law fluid flow in parallel plates duct. The problem was solved using an approximate analytical solution. The developing heat transfer problem was solved assuming fully developed fluid flow. Both problems were solved using the integral form of the momentum and energy equations.

Al-Ali [35] and Al-Ali and Selim [36] used the integral boundary layer method to solve the simultaneously developing Newtonian fluid flow and heat transfer in a circular tube subject to a uniform heat flux. The thermal entrance length was assumed to have two regions, the thermal inlet region and the thermally filled region. As the thermal boundary layer edge reaches the tube axis, the temperature profile is not fully developed yet. Therefore, an inlet filled region concept [8] was assumed with the fully developed profile asymptotically attained. The result reported in their study was novel in the context that developing profiles asymptotically reached the fully developed values. The results were validated by comparison with results from the literature for the Newtonian fluid flow case.

Chebbi [5] addressed the problem of hydrodynamic developing power-law fluid flow in the entrance region of a circular pipe using Ishizawa's [8] inlet-filled region concept along with an integral boundary layer method. The obtained results included different

profiles: hydrodynamic boundary layer thickness, shape factor, local friction factor, centerline velocity profile, pressure drop in addition to inlet and entrance length sizes for different power law indices. The results were validated against available published results in the literature for different power law indices and n=1 (Newtonian fluid flow as a special case).

Chapter 3. Methodology

3.1. Governing Equations

Ishizawa's concept of the hydrodynamic inlet-filled region [8] for axisymmetric flow between parallel disks is extended in the current study. The developed model for power-law fluids uses the hydrodynamic entrance region model developed in [5] for power-law fluids and extends the heat transfer model presented in [35, 36] for the Newtonian fluid flow case. The analysis requires derivation of the integral energy equation and finding an approximate temperature profile to find the relevant parameters in the inlet and filled regions. The solution is expected to provide the local Nusselt number in the entrance region that asymptotically approaches the fully developed temperature profile. The results will be compared with available solutions in the literature.

Laminar fluid flow is considered to occur in the entrance region of a circular pipe having a radius *R* shown in Figure 1. The power-law fluid is characterized by its power-law index *n* and a consistency coefficient *K* [37]. The analysis covers fluids with constant relevant properties with incompressible flow, assuming uniform velocity and temperature profiles at the entrance of the pipe. The continuity (equation (3), momentum (equation (4), and energy (equation (6) equations in cylindrical coordinates with r and x being radial and axial coordinates, respectively, can thus be written as [38]:

$$\frac{\partial}{\partial r}(rv) + \frac{\partial}{\partial x}(ru) = 0 \tag{3}$$

$$u\frac{\partial u}{\partial x} + v\frac{\partial u}{\partial r} = -\frac{K}{\rho}\frac{1}{r}\frac{\partial}{\partial r}\left[r\left(-\frac{\partial u}{\partial r}\right)^{n}\right] - \frac{1}{\rho}\frac{\partial P}{\partial x} \tag{4}$$

$$\frac{\partial P}{\partial r} = 0 \tag{5}$$

$$\rho\hat{\mathrm{C}}_p\left(v\frac{\partial T}{\partial r} + u\frac{\partial T}{\partial x}\right) = k\left[\frac{1}{r}\frac{\partial}{\partial r}\left(r\frac{\partial T}{\partial r}\right)\right] \tag{6}$$

where, u and v are velocity components in the x and r directions, respectively, ρ is density, P is the pressure, $\hat{\mathrm{C}}_p$ is heat capacity per unit mass at constant pressure, T is temperature, and k is the thermal conductivity.

The boundary conditions for equations (3) to (5) are given elsewhere [5]:

To solve thermal inlet region problem, the following boundary conditions are used for equation (6)

$$\begin{array}{ll} \text{at } r = R & \text{at } r = R - \delta_T \\ v = 0 & T = T_o \\ q_o = k\,\partial T/\partial r & {}^{dT}/_{dr} = 0 \end{array} \qquad (7)$$

To solve the thermally filled region, the following boundary conditions are used for equation (6)

$$\begin{array}{ll} rR & v = 0 \\ r = R & {}^{dT}/_{dr} = {}^{q_0}/_{k} \end{array} \qquad (8)$$

Here, we consider the steady state case. Moreover, we neglect the viscous dissipation, and axial conduction as compared to axial convection, in relation to Brinkman and Péclet numbers.

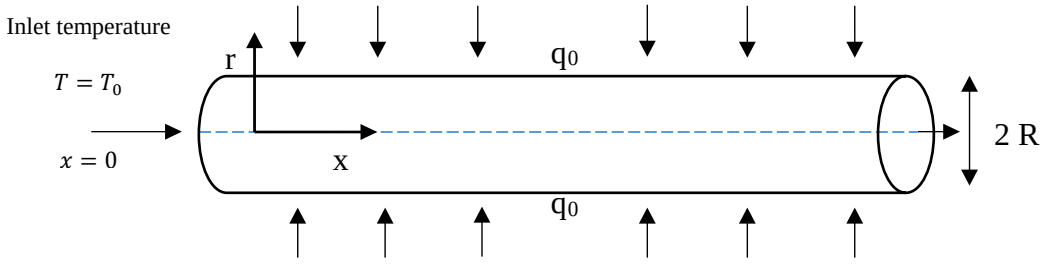

Figure 1: Schematic representation of the constant heat flux q_0 condition at r = R

3.2. Analysis of the Temperature Field

The inlet-filled region approach by Ishizawa [8] was successfully used to solve the entrance region hydrodynamic problem for Newtonian fluid flow [6] and power-law fluid flow [5] in circular pipes. This success warrants its application on power-law fluids under simultaneously developing hydrodynamic and thermal boundary layers at constant wall heat-flux. A constant wall heat-flux is maintained at the pipe wall. We consider the case of Prandtl (Pr) larger than one, which applies to ordinary liquids [38].

The solution for the case Pr less than one and Newtonian fluids can be found in [35,36]. Gases (Newtonian fluids) and liquid metals (if treated as Newtonian) fall in this category.

In the case Pr larger than one (power-law ordinary liquids) considered in this investigation, thermal boundary layer thickness (δ_T) is less than hydrodynamic boundary layer thickness (δ) and the entrance region includes three zones: a hydrodynamic inlet – thermal inlet region followed by a hydrodynamic filled and finally a hydrodynamic filled – thermally filled region.

3.3. Thermal Inlet Region

Equations (3) and (6) can be used together using the previously mentioned boundary conditions yield the following result for the thermal inlet region $\left(0 < x < L_{in,T}\right)$ as in [30].

$$\frac{d}{dx}\left[\delta_T \int_0^{\delta_T} \frac{(T - T_0)}{q\delta_T/k} u\left(1 - \frac{y}{R}\right) dy\right] = \alpha \tag{9}$$

Where, aproximate temperature (*T*) and velocity profiles (*u)* are function of *x*. The dimensionless form of Equation (9) is given in subsequent sections.

3.4. Inlet Region Temperature Profile

For the constant heat flux, the following dimensionless approximate quadratic temperature profile is used:

$$T^* = b_0 + b_1\eta_T + b_2\eta_T^2 + b_3\eta_T^3 + b_4\eta_T^{q+2} \tag{10}$$

where $T^* = \frac{T-T_0}{q\delta_T/k}$, $\eta_T = {}^{y}/_{\delta_T}$, $q = 1 + \frac{1}{n}$ and $b_0 - b_4$ are functions of x only.

In the thermal inlet region $\left(0 < x < L_{in,T}\right)$ it is possible to set $\frac{\partial T^*}{\partial \eta_T}$ and $\frac{\partial^2 T^*}{\partial \eta_T^2} = 0$, because the fluid outside thermal boundary layer has a uniform temperature. Therefore, the boundary conditions for this region can be written as follows to solve for the coefficients $b_0 - b_4$:

At $\eta_T = 1$	At $\eta_T = 0$:
$T^* = 0$	$\frac{\partial T^*}{\partial \eta_T} = -1$
$\frac{\partial T^*}{\partial \eta_T} = 0$	$\frac{\partial^2 T^*}{\partial \eta_T^2} = -\bar{\delta}_T$
$\frac{\partial^2 T^*}{\partial \eta_T^2} = 0$	

Using MATLAB to solve for the coefficients in 3.8 yields the following dimensionless temperature profile.

$$T^* = \frac{4p-4}{6p} - \eta_T + \frac{p-1}{3p-9}{\eta_T}^3 + \frac{2}{-p^2+3p}{\eta_T}^p + \left[\frac{p-2}{6p} - \frac{1}{2}{\eta_T}^2 + \frac{p-2}{3p-9}{\eta_T}^3 + \frac{1}{-p^2+3p}{\eta_T}^p\right]\bar{\delta}_T \quad (11)$$

3.5. Thermally Filled Region

In the thermally filled region $(x > L_{in,T})$, the dimensionless thermal boundary layer thickness $\bar{\delta}_T$ is equal to 1; in other words, δ_T is identically equal to the pipe radius. Equations (3) and equation (6) can be solved together using the abovementioned boundary conditions. This yields as in [29]

$$\frac{d}{dx}\int_0^R u.\frac{(T-T_c)}{q/k}\left(1-\frac{y}{R}\right)dy = \alpha\left[1 - \frac{U_0}{U_c}\Gamma_T\right] \quad (12)$$

The dimensionless form of equation (12) is given in subsequent sections. In this region, the centerline temperature T_c does not remain constant due the propagation of heat effects throughout the cross-section of the pipe. Therefore, at the outer edge of thermal boundary layer, along the pipe centerline at $y = \delta_T = R$, $\frac{\partial T^*}{\partial \eta_T} = 0$ due to symmetry while $\frac{\partial^2 T^*}{\partial \eta_T^2}$ isn't equal to zero.

3.6. Filled Region Temperature Profile

In the filled region, the following dimensionless boundary conditions are used to solve equation (10):

At $\eta_T = 1$	At $\eta_T = 0$:
$T^* = 0$	$\frac{\partial T^*}{\partial \eta_T} = -1$
$\frac{\partial T^*}{\partial \eta_T} = 0$	$\frac{\partial^2 T^*}{\partial \eta_T^2} = -1$
$\frac{\partial^2 T^*}{\partial \eta_T^2} = \Gamma_T$	

Using MATLAB to solve for the coefficients in equation (10) yields the following dimensionless temperature profile.

$$T^* = \frac{5p-6}{6p} - \eta_T - \frac{1}{2}{\eta_T}^2 + \frac{2p-3}{3p-9}{\eta_T}^3 + \frac{3}{3p-p^2}{\eta_T}^p + \Gamma_T\left(-\frac{{\eta_T}^p}{3p-p^2} - \frac{{\eta_T}^3}{3p-9} + \frac{1}{3p}\right) \quad (13)$$

For Newtonian fluids ($n = 1$) , Γ_T asymptotically reaches 2. Moreove, general temperature profile given by equation (13) takes the shape of the fully developed temperature profile at appropriate values of Γ_T.

Table 3.1: Coefficients of the approximate thermal profile

	Inlet region	Filled region
b_0	$-\frac{4-4p+2\bar{\delta}_T-\bar{\delta}_T p}{6p}$	$\frac{5p+2\Gamma_T-6}{6p}$
b_1	-1	-1
b_2	$-\bar{\delta}_T/2$	$-1/2$
b_3	$-\frac{1-p+2\bar{\delta}_T-\bar{\delta}_T p}{3(-3+p)}$	$-\frac{-2p+\Gamma_T+3}{3(-3+p)}$
b_4	$\frac{2+\bar{\delta}_T}{3p-p^2}$	$-\frac{\Gamma_T-3}{3p-p^2}$

where $\bar{\delta}_T = \delta_T \,/\, R$, and $p = q + 2$.

Table 3.2.Coefficients of the approximate velocity profile [5]

	Inlet region	Filled region
ζ	$\zeta = 1 - y/\delta$	$\zeta = 1 - y/R \ = r/R$
a_1	0	$\frac{\alpha + 2\Gamma - \lambda + n(-2 + 2\alpha - 3q + 2\alpha q - q^2)}{2n}$
a_2	$\frac{-2n - 3nq - nq^2 - (q+2)\bar{\delta} + \lambda}{2n + 2nq + \bar{\delta}}$	$\frac{-\alpha - 2\Gamma + \lambda + n(-\alpha + 2q - 2\alpha q + q^2)}{n}$
a_3	$\frac{nq + nq^2 + (q+1)\bar{\delta} - \lambda}{2n + 2nq + \bar{\delta}}$	$\frac{\alpha + 2\Gamma - \lambda + n(-q + 2\alpha q - q^2)}{2n}$

3.7. Fully Developed Temperature Profile – Power Law Fluids

The constant heat flux problem for Newtonian fluids [38] is extended to power law fluids by [38] solving the following equation for ε^q instead of ε^2.

$$(1 - \varepsilon^q)\frac{\partial T^*}{\partial \chi} = \frac{1}{\varepsilon}\frac{\partial}{\partial \varepsilon}\left(\varepsilon \frac{\partial T^*}{\partial \varepsilon}\right) \tag{14}$$

where

$$T^* = \frac{T - T_0}{q_0 R/k},\ \varepsilon = \frac{r}{R},\ \chi = \frac{x}{\rho \hat{C}_p u_{max} R^2/k} \tag{15}$$

The following boundary conditions are used to solve equation (15)

$$\begin{aligned} &\text{B.C. 1:} && \varepsilon = 0 && T^* = finite \\ &\text{B.C. 2:} && \varepsilon = 1 && \frac{\partial T^*}{\partial \varepsilon} = 1 \\ &\text{B.C. 3:} && \chi = 0 && T^* = 0 \end{aligned} \tag{16}$$

$$\chi = \int_0^1 T^*(\chi, \varepsilon)(1 - \varepsilon^q)\varepsilon d\varepsilon$$

For large χ one can assume a solution of the following form:

$$T^*(\chi, \varepsilon) = C_0 \chi + \Psi(\varepsilon) \tag{17}$$

Simplification yields,

$$\frac{1}{\varepsilon}\frac{d}{d\varepsilon}\left(\varepsilon \frac{d\Psi}{d\varepsilon}\right) = C_0(1 - \varepsilon^q) \tag{18}$$

Integration of the equation twice with respect to ε and substituting into equation (17) gives:

$$T^*(\chi,\varepsilon) = C_0\chi + C_0\left(\frac{\varepsilon^2}{4} - \frac{\varepsilon^{q+2}}{(q+2)^2}\right) + C_1\ln(\varepsilon) + C_2 \tag{19}$$

Three constants are determined from boundary conditions 1, 2, and 4.

$$C_1 = 0$$

$$C_0 = \frac{2(q+2)}{q} \tag{20}$$

$$C_2 = -\frac{(q^3+6q^2+12q)}{2q(q+4)(2q+4)}$$

Substitution of these constants in equation (19**)** and simplification yield

$$T^*(\chi,\varepsilon) = \frac{2(q+2)}{q}\chi + \frac{2(q+2)}{q}\left(\frac{\varepsilon^2}{4} - \frac{\varepsilon^{q+2}}{(q+2)^2}\right) - \frac{(q^3+6q^2+12q)}{2q(q+4)(2q+4)} \tag{21}$$

The results are found consistent with those of Bird [27].

3.8. Derivation of Equations Required to Solve the Heat Transfer

The equations leading to the solution of the heat transfer problem in the three zones forming the entrance region are presented in this section.

3.8.1. Hydrodynamic inlet – thermal inlet

In this region, equation (9) can be written in dimensionless form as follows:

$$d\left[\bar{U}_\infty\bar{\delta}_T^2\int_0^1 \bar{u}\,T^*\left(1-\eta_T\bar{\delta}_T\right)d\eta_T\right] = \frac{2}{Pr}\,d\xi \tag{22}$$

where.

$$T^* = \frac{T-T_0}{q\delta_T/k}, \bar{u} = \frac{u}{U_\infty}, \bar{U}_\infty = \frac{U_\infty}{U_0}, \eta_T = \frac{y}{\delta_T}, \xi = \frac{x}{RRe}, \bar{\delta}_T = \frac{\delta_T}{R}, Pr = \frac{U_0(2R)}{\alpha Re} \tag{23}$$

To solve equation (22), approximate temperature and velocity profiles are substituted. The velocity profile in [5] is used:

$$\bar{u} = 1 + \zeta^q(a_1 + a_2\zeta + a_3\zeta^2) \tag{24}$$

However, before substitution of the velocity profile an appropriate modification is made using

$$\zeta = 1 - \frac{y}{\delta} \tag{25}$$

For the inlet region temperature profile, we know that:

$$\eta_T = \frac{y}{\delta_T} \tag{26}$$

Therefore:

$$\zeta = 1 - \eta_T \frac{\bar{\delta}_T}{\bar{\delta}} \tag{27}$$

Substituting for ζ given in equation (27) into equation (24) yields after simplification:

$$\bar{u} = 1 + \left(1 - \eta_T\bar{\delta}_T/\bar{\delta}\right)^q(A_1 + A_2\eta_T + A_3{\eta_T}^2) \tag{28}$$

where:

$$A_1 = a_1 + a_2 + a_3 \tag{29}$$

$$A_2 = -(a_2 + 2a_3)\bar{\delta}_T/\bar{\delta} \tag{30}$$

$$A_3 = a_3\left(\bar{\delta}_T/\bar{\delta}\right)^2 \tag{31}$$

The integral term in equation (22) is obtained using MATLAB by substituting equations (11) and (44) with the appropriate coefficients given in Table 3.2. This yields a differential equation. For n=1 [35], the result is as follows

$$\frac{d}{d\xi}\left[\bar{U}_\infty\left(\left(-\frac{a_3}{2160\,\delta^4}\right)\delta_T^8+\left(\frac{a_2}{1260\,\delta^3}+\frac{a_3}{315\,\delta^3}-\frac{a_3}{1260\,\delta^4}\right)\delta_T^7\right.\right.$$
$$+\left(\frac{13\,a_2}{10080\,\delta^3}-\frac{a_3}{112\delta^2}-\frac{a_2}{224\,\delta^2}+\frac{13\,a_3}{2520\,\delta^3}\right.$$
$$\left.+\frac{a_3}{360\,\delta^4}\right)\delta_T^6$$
$$+\left(\frac{a_2}{105\,\delta}+\frac{4\,a_3}{315}-\frac{11\,a_2}{1680\,\delta^2}-\frac{11\,a_3}{840\,\delta^2}-\frac{3\,a_2}{560\,\delta^3}\right.$$
$$\left.-\frac{3\,a_3}{140\,\delta^3}\right)\delta_T^5 \qquad (32)$$
$$+\left(\frac{3\,a_2}{280\,\delta}-\frac{a_3}{120}-\frac{a_2}{120}+\frac{a_3}{70\,\delta}+\frac{a_2}{28\,\delta^3}+\frac{a_3}{14\,\delta^3}\right.$$
$$\left.-\frac{1}{120}\right)\delta_T^4+\left(-\frac{a_2}{10\,\delta}-\frac{2\,a_3}{15\,\delta}\right)\delta_T^3$$
$$\left.+\left(\frac{3\,a_2}{20}+\frac{3\,a_3}{20}+\frac{3}{20}\right)\delta_T^2\right)\Bigg]=\frac{2}{Pr}$$

3.8.2. Hydrodynamic filled - thermal inlet region

In this region, equation (9) can be written in dimensionless form as follows:

$$d\left[\bar{U}_c\bar{\delta}_T^2\int_0^1\bar{u}\,T^*\left(1-\eta_T\bar{\delta}_T\right)d\eta_T\right]=\frac{2}{Pr}\,d\xi \qquad (33)$$

where

$$T^*=\frac{T-T_0}{q\delta_T/k},\ \bar{u}=\frac{u}{U_c},\ \bar{U}_c=\frac{U_c}{U_0},\ \eta_T=\frac{y}{\delta_T},\ \xi=\frac{x}{RRe},\ \bar{\delta}_T=\frac{\delta_T}{R},\ Pr=\frac{U_0(2R)}{\alpha Re} \qquad (34)$$

To solve (33), appropriate temperature and velocity profiles are substituted. The velocity profile [5] is given by:

$$\bar{u}=1+\zeta^q(a_1+a_2\zeta+a_3\zeta^2) \qquad (35)$$

However, before substitution of velocity profile an appropriate modification was made as follows:

$$\zeta=1-\frac{y}{R} \qquad (36)$$

For the inlet region temperature profile, we know that:

$$\eta_T=\frac{y}{\delta_T} \qquad (37)$$

Therefore ζ will becomes:

$$\zeta = 1 - \eta_T \bar{\delta}_T \tag{38}$$

where: $\bar{\delta}_T = \delta_T / R$

Substituting for ζ given in equation (38) into equation (35) yields after simplification:

$$\bar{u} = 1 + \left(1 - \eta_T \bar{\delta}_T\right)^q (A_1 + A_2 \eta_T + A_3 {\eta_T}^2) \tag{39}$$

where:

$$A_1 = a_1 + a_2 + a_3 \tag{40}$$

$$A_2 = -(a_2 + 2a_3)\bar{\delta}_T \tag{41}$$

$$A_3 = a_3 {\bar{\delta}_T}^2 \tag{42}$$

The integral term in equation (22) is obtained using MATLAB by substituting equations (11) and (44) with the appropriate coefficients given in Table 3.2. This yields a differential equation. For n=1 [35], the result is as follows

$$\begin{aligned} \frac{d}{d\xi}\Bigg[\bar{U}_c \Bigg(& \left(-\frac{a_3}{2160}\right)\delta_T^8 + \left(\frac{a_2}{1260} + \frac{a_3}{420}\right)\delta_T^7 \\ & + \left(-\frac{a_1}{672} - \frac{a_2}{315} - \frac{a_3}{1008}\right)\delta_T^6 \\ & + \left(\frac{a_1}{240} - \frac{a_2}{420} - \frac{11\,a_3}{504}\right)\delta_T^5 \\ & + \left(\frac{3\,a_1}{280} + \frac{4\,a_2}{105} + \frac{13\,a_3}{168} - \frac{1}{120}\right)\delta_T^4 \\ & + \left(-\frac{a_1}{15} - \frac{a_2}{10} - \frac{2\,a_3}{15}\right)\delta_T^3 \\ & + \left(\frac{3\,a_1}{20} + \frac{3\,a_2}{20} + \frac{3\,a_3}{20} + \frac{3}{20}\right)\delta_T^2 \Bigg)\Bigg] = \frac{2}{Pr} \end{aligned} \tag{43}$$

3.8.3. Hydrodynamic filled – thermally filled region

Equation (12) can be written in dimensionless form as follows

$$d\left[\bar{U}_c \int_0^1 T^* \bar{u}\,(1 - \eta_T) d\eta_T\right] = \frac{2}{Pr}\left[1 - \frac{\Gamma_T}{\bar{U}_c}\right] d\xi \tag{44}$$

where:

$$T^* = \frac{T-T_c}{qR/k}, \bar{u} = \frac{u}{U_c}, \bar{U}_c = \frac{U_c}{U_0}, \eta_T = \frac{y}{R}, \xi = \frac{x}{RRe}, Pr = \frac{U_0(2R)}{\alpha Re} \quad (45)$$

To solve equation (44), appropriate temperature and velocity profiles are substituted. The velocity profile is obtained from [5] and is given as follows:

$$\bar{u} = 1 + \zeta^q(a_1 + a_2\zeta + a_3\zeta^2) \quad (46)$$

For the filled region hydrodynamic profile, we know that:

$$\zeta = 1 - \frac{y}{R} \quad (47)$$

with

$$\eta_T = \frac{y}{R} \quad (48)$$

Therefore ζ can be written as:

$$\zeta = 1 - \eta_T \quad (49)$$

Substituting for ζ given in equation (49) into equation (46) and gives after simplification:

$$\bar{u} = 1 + (1 - \eta_T)^q(A_1 + A_2\eta_T + A_3{\eta_T}^2) \quad (50)$$

where:

$$A_1 = a_1 + a_2 + a_3 \quad (51)$$

$$A_2 = -(a_2 + 2a_3) \quad (52)$$

$$A_3 = a_3 \quad (53)$$

The integral term in equation (22) is obtained using MATLAB by substituting equations (10) and (13) and with the appropriate coefficients given in Table 3.2. This yields a differential equation. For n=1 [35], the result is as follows (54)

$$\frac{d}{d\xi}\left[\bar{U}_c\left(\left(\frac{13\,a_1}{672}+\frac{a_2}{63}+\frac{29\,a_3}{2160}+\frac{1}{30}\right)\Gamma_T-\frac{215\,a_1}{672}-\frac{a_2}{4}-\frac{221\,a_3}{1080}-\frac{83}{120}\right)\right]=\frac{2}{Pr}\left[1-\frac{\Gamma_T}{\bar{U}_c}\right]$$

3.9. Nusselt Number

The Nusselt number can be written as:

$$Nu=\frac{hD_e}{k} \tag{55}$$

where the equivalent diameter D_e is equal to $2R$.

The heat transfer coefficient h is defined as:

$$h=-\frac{k}{T_w-T_b}\frac{\partial T}{\partial y}\,|_{y=0} \tag{56}$$

where, $\frac{\partial T}{\partial y}\,|_{y=0}=-\frac{q}{k}$

Simplification of equation (55) yields

$$Nu=\frac{2R}{T_w-T_b}\frac{q}{k} \tag{57}$$

Multiplication of δ_T/δ_T with equation (57) and simplification yield:

$$Nu=\frac{2}{\left(\frac{T_w-T_b}{q\delta_T/k}\right)\bar{\delta}_T} \tag{58}$$

Using the inlet region temperature profile equation (11) at $y=0$ gives:

$$T_w-T_b=\left[\frac{4p-4}{6p}+\frac{p-2}{6p}\bar{\delta}_T\right].\frac{q\delta_T}{k} \tag{59}$$

where: $\bar{\delta}_T=\frac{\delta_T}{R}$

The bulk temperature is given by [35]:

$$T_b-T_o=\frac{\int_0^R u(T-T_o)rdr}{\int_0^R rudr} \tag{60}$$

where: $\int_0^R rudr=\frac{R^2U_o}{2}$

Changing coordinates for the numerator in equation (60) gives.

$$\int_0^R u(T-T_o)rdr = R\int_0^R u(T-T_o)\left(1-\frac{y}{R}\right)dy \tag{61}$$

Simplification of equation (60) yields [35]:

$$T_b - T_o = \frac{2}{RU_o}\int_0^R u(T-T_o)\left(1-\frac{y}{R}\right)dy \tag{62}$$

Subtracting equation (59) from equation (62) gives after simplification:

$$T_w - T_b = \frac{\left[\frac{4p-4}{6p}+\frac{p-2}{6p}\bar{\delta}_T\right]q\delta_T}{k} - \frac{2}{RU_o}\int_0^R u(T-T_o)\left(1-\frac{y}{R}\right)dy \tag{63}$$

3.9.1. Hydrodynamic inlet – thermal inlet

In this region, equation (63) can be written in dimensionless form as follows:

$$\frac{(T_w - T_b)}{q\delta_T/k} = \left[\frac{4p-4}{6p}+\frac{p-2}{6p}\bar{\delta}_T\right] - 2\bar{U}_\infty\bar{\delta}_T\int_0^1 \bar{u}\,T^*\left(1-\eta_T\bar{\delta}_T\right)d\eta_T \tag{64}$$

where:

$$T^* = \frac{T-T_0}{q\delta_T/k},\ \bar{u} = \frac{u}{U_\infty},\ \bar{U}_\infty = \frac{U_\infty}{U_0},\ \eta_T = \frac{y}{\delta_T},\ \bar{\delta}_T = \frac{\delta_T}{R}, \tag{65}$$

This yields the following expression for the Nusselt number

$$Nu = \frac{2}{\bar{\delta}_T\left(\left[\frac{4p-4}{6p}+\frac{p-2}{6p}\bar{\delta}_T\right] - 2\bar{U}_\infty\bar{\delta}_T\int_0^1 \bar{u}\,T^*\left(1-\eta_T\bar{\delta}_T\right)d\eta_T\right)} \tag{66}$$

3.9.2. Hydrodynamic filled - thermal inlet region

In this region, equation (63) can be written in dimensionless form as follows:

$$\frac{(T_w - T_b)}{q\delta_T/k} = \left[\frac{4p-4}{6p}+\frac{p-2}{6p}\bar{\delta}_T\right] - 2\bar{U}_c\bar{\delta}_T\int_0^1 \bar{u}\,T^*\left(1-\eta_T\bar{\delta}_T\right)d\eta_T \tag{67}$$

where:

$$T^* = \frac{T-T_0}{q\delta_T/k},\ \bar{u} = \frac{u}{U_c},\ \bar{U}_c = \frac{U_c}{U_0},\ \eta_T = \frac{y}{\delta_T},\ \bar{\delta}_T = \frac{\delta_T}{R}, \tag{68}$$

This yields the following expression for the Nusselt number

$$Nu = \frac{2}{\bar{\delta}_T \left(\left[\frac{4p-4}{6p} + \frac{p-2}{6p} \bar{\delta}_T \right] - 2\bar{U}_c \bar{\delta}_T \int_0^1 \bar{u}\, T^* \left(1 - \eta_T \bar{\delta}_T\right) d\eta_T \right)} \tag{69}$$

3.9.3. Hydrodynamic filled - thermal filled region

In this region, equation (63) can be modified for the filled region by replacing the inlet region temperature profile with the filled region one. This yields the following:

$$\frac{(T_w - T_b)}{q\delta_T/k} = \left[\frac{5p + 2\Gamma_T - 6}{6p} \right] - 2\bar{U}_c \int_0^1 \bar{u}\, T^* \left(1 - \eta_T \bar{\delta}_T\right) d\eta_T \tag{70}$$

where:

$$T^* = \frac{T - T_c}{qR/k}, \bar{u} = \frac{u}{U_c}, \bar{U}_c = \frac{U_c}{U_0}, \eta_T = \frac{y}{R}, \ \bar{\delta}_T = \frac{\delta_T}{R} = 1, \tag{71}$$

Therefore, the Nusselt number is given by

$$Nu = \frac{2}{\left(\left[\frac{5p + 2\Gamma_T - 6}{6p} \right] - 2\bar{U}_c \int_0^1 \bar{u}\, T^* (1 - \eta_T) d\eta_T \right)} \tag{72}$$

Chapter 4. Results and Analysis

4.1. Method of Solution

Solution of the simultaneously developing power-law fluid flow and heat transfer is performed by integrating the following differential equations to solve for δ and λ and δ_T using a variable step fourth order Runge-Kutta (RK4) and FORTRAN programming

$$\frac{d\bar{\delta}}{d\xi} = \frac{F_{1i}G_{22i} - F_{2i}G_{12i}}{G_{11i}G_{22i} - G_{21i}G_{12i}} \tag{73}$$

$$\frac{d\lambda}{d\xi} = \frac{F_{2i}G_{11i} - F_{1i}G_{21i}}{G_{11i}G_{22i} - G_{21i}G_{12i}} \tag{74}$$

$$\frac{d\bar{\delta}_T}{d\xi} = \frac{F_{3i} - G_{31i} * \frac{d\bar{\delta}}{d\xi} - G_{32i} * \frac{d\lambda}{d\xi}}{G_{33i}} \tag{75}$$

where the variables in equation (73) and equation (74) are obtained from [5] with:

$F_{3i} = \frac{2}{Pr}$, $G_{31i} = \frac{\partial\bar{\delta}_{3i}}{\partial\Gamma}$, $G_{32i} = \frac{\partial\bar{\delta}_{3i}}{\partial\lambda}$, $G_{33i} = \frac{\partial\bar{\delta}_{3i}}{\partial\bar{\delta}_T}$, $\bar{\delta}_{3i} = \bar{U}_\infty\bar{\delta}_T^2\int_0^1 \bar{u}\,T^*\left(1-\eta_T\bar{\delta}_T\right)d\eta_T$

The initial value for ξ was set at 10^{-6} and the solution was obtained for its increasing values until $\bar{\delta} = 1$ at which point $\xi = \xi_{in,H}$ marks the end of the hydrodynamic inlet region. Moreover, the local Nusselt number was obtained by using equation (64).

For the zone that follows i.e., hydrodynamic filled – thermal inlet region, the following three equations were solved simultaneously

$$\frac{d\Gamma}{d\xi} = \frac{F_{1f}G_{22f} - F_{2f}G_{12f}}{G_{11f}G_{22f} - G_{21f}G_{12f}} \tag{76}$$

$$\frac{d\lambda}{d\xi} = \frac{F_{2f}G_{11f} - F_{1f}G_{21f}}{G_{11f}G_{22f} - G_{21f}G_{12f}} \tag{77}$$

$$\frac{d\bar{\delta}_T}{d\xi} = \frac{F_{3i} - G_{31i} * \frac{d\Gamma}{d\xi} - G_{32i} * \frac{d\lambda}{d\xi}}{G_{33i}} \tag{78}$$

where the variables in equation (76) and equation (77) are obtained from [5] while:

$F_{3i} = \frac{2}{Pr}$, $G_{31i} = \frac{\partial \bar{\delta}_{3i}}{\partial \Gamma}$, $G_{32i} = \frac{\partial \bar{\delta}_{3i}}{\partial \lambda}$, $G_{33i} = \frac{\partial \bar{\delta}_{3i}}{\partial \bar{\delta}_T}$, $\bar{\delta}_{3i} = \bar{U}_c \bar{\delta}_T^2 \int_0^1 \bar{u}\, T^* \left(1 - \eta_T \bar{\delta}_T\right) d\eta_T$

The starting value of Γ was set to zero and the equations were solved until $\bar{\delta}_T = 1$. This point marks the end of thermal inlet region. Moreover, local Nusselt number was obtained by using equation (69).

For the third region i.e., hydrodynamic filled – thermal filled region, the following three equations were solved simultaneously

$$\frac{d\Gamma}{d\xi} = \frac{F_{1f} G_{22f} - F_{2f} G_{12f}}{G_{11f} G_{22f} - G_{21f} G_{12f}} \tag{79}$$

$$\frac{d\lambda}{d\xi} = \frac{F_{2f} G_{11f} - F_{1f} G_{21f}}{G_{11f} G_{22f} - G_{21f} G_{12f}} \tag{80}$$

$$\frac{d\Gamma_T}{d\xi} = \frac{F_{3f} - G_{31f} * \frac{d\Gamma}{d\xi} - G_{32f} * \frac{d\lambda}{d\xi}}{G_{33f}} \tag{81}$$

where the variables in equation (79) and equation (80) are obtained from [5] while:

$F_{3f} = \frac{2}{Pr}\left[1 - \frac{\Gamma_T}{\bar{U}_c}\right]$, $G_{31f} = \frac{\partial \bar{\delta}_{3f}}{\partial \Gamma}$, $G_{32f} = \frac{\partial \bar{\delta}_{3f}}{\partial \lambda}$, $G_{33f} = \frac{\partial \bar{\delta}_{3f}}{\partial \bar{\delta}_T}$,

$\bar{\delta}_{3f} = \bar{U}_c \int_0^1 \bar{u}\, T^* (1 - \eta_T) d\eta_T$

The starting value of Γ_T was set to zero and the equations were solved until Γ_T reaches its asymptotic values for each power-law index, 2 for $n = 1$. The location, ξ_T , at which the Nusselt number reaches 1.05 times the asymptotic value marks the end of the thermal entrance region. Moreover, the local Nusselt number was obtained by solving equation (70).

4.2. Results and discussion

Figure 4-1 through Figure 4-9 show heat transfer results and selected data is presented in Table 4.1 through Table 4.6. Figure 4-1 through Figure 4-3 show the variation of the thermal boundary layer thickness with axial distance for Prandtl numbers 1 – 15 and power-law index n from 0.6 – 1.4. The hydrodynamic boundary layer thickness $\bar{\delta}$ for the different values of n are plotted for comparison. The axial distance $\xi_{in,T}$, at which $\bar{\delta}_T = 1$ are tabulated as function of Prandtl number in Table 4.1, Table 4.3 and Table

4.5 for $n = 0.6, 1$ and 1.4, respectively. At this location, the thermal boundary layer thickness reaches the pipe axis and marks the end of the thermal inlet region. An increase of the thermal inlet length can be observed with increasing Prandtl number for example for $n = 0.6$ at Pr $= 1$, $\xi_{in,T} = 0.055$ while it is $\xi_{in,T} = 0.787$ for Pr $= 15$.

Figure 4-4 through Figure 4-6 show the variation in thermal shape factor Γ_T along the axial distance ξ for $n = 0.6, 1\ and\ 1.4$, respectively. Γ_T is zero in the thermal inlet region and increases in the thermally filled region. For all values of n, Γ_T asymptotically reaches the fully developed value.

Figure 4-7 through Figure 4-9 show the trends for the local Nusselt number for different Prandtl number for $n = 0.6 - 1.4$. For $n = 1$, the local Nusselt number asymptotically approaches 4.36. At low Prandtl number, the Nusselt number nearly reaches its asymptotic value, at smaller ξ. This is true for all power-law indices. This trend indicates that fluids with low Prandtl reach their fully developed heat transfer state faster compared to fluids with high Prandtl. These figures are also useful in determining the pipe length at which thermal profile reaches its fully developed condition. The thermal entrance length ξ_T is the heated length of a pipe required for the local Nusselt number to reach within 5% of its fully developed value. It is 48/11 or 4.36 for $n = 1$. The values of the thermal entrance region size ξ_T and the thermally filled region size $\xi_T - \xi_{in,T}$ lengths are listed in in Table 4.7 to Table 4.9. ξ_T is calculated using the Nusselt number criterion, for the three power-law indices, namely 0.6, 1 and 1.4 against Prandtl number between 1 to 15. The thermally filled region occupies between 18 – 25 % of the total thermal entrance length for $n = 0.6$ however, it reaches 46% when $n = 1.4$. This confirms the importance of the thermal filled region and thus its consideration in heat transfer analysis especially for fluids having higher power-law indices.

Figure 4-10 through Figure 4-12 present a comparison of the numerical results for the thermal boundary layer thickness, local Nusselt number, and thermal shape factor respectively, with results presented in [35]. Throughout the thermal entrance length, the results of the current analysis and the numerical analysis of [35] show good agreement.

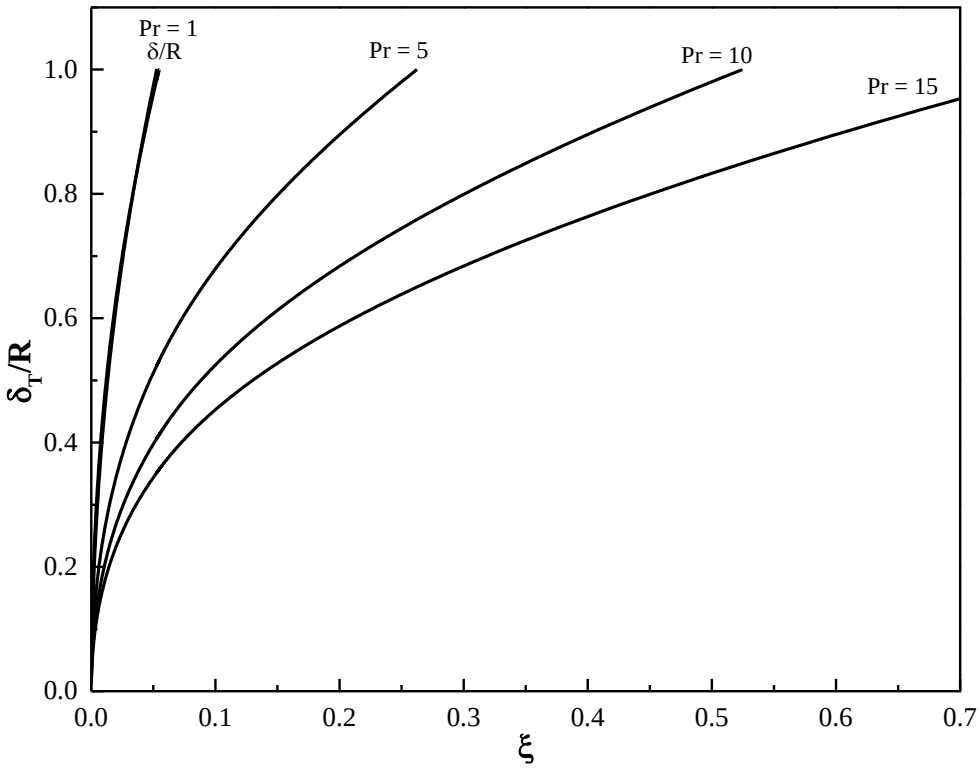

Figure 4-1. Hydrodynamic and Thermal Boundary Layer Thicknesses for Different Prandtl Numbers at *n = 0.6*

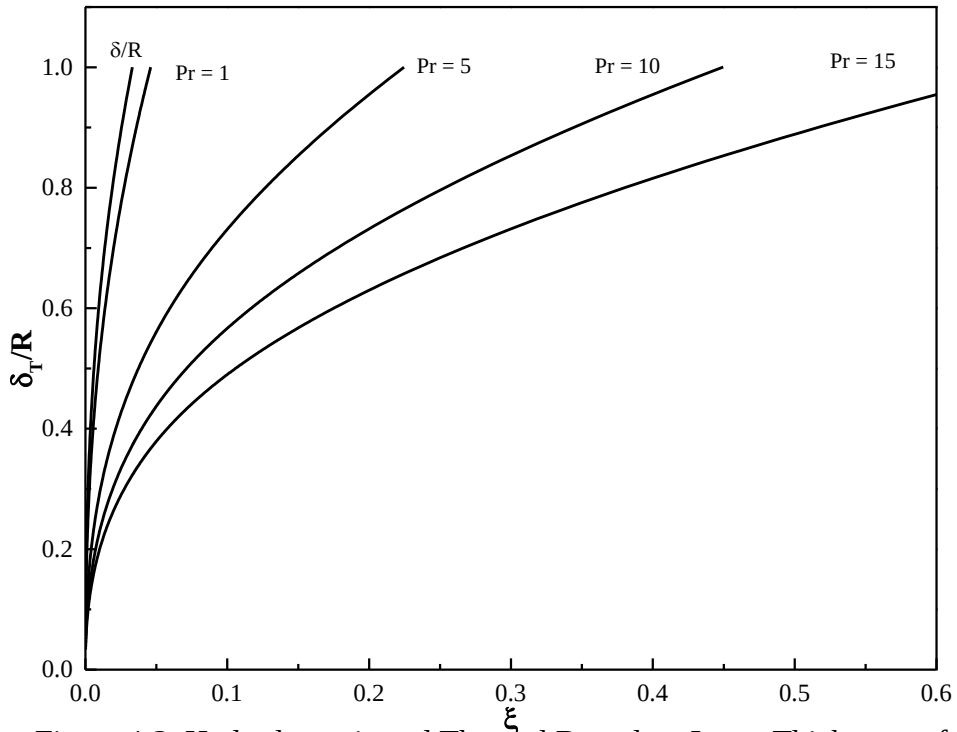

Figure 4-2. Hydrodynamic and Thermal Boundary Layer Thicknesses for Different Prandtl Numbers at *n = 1*

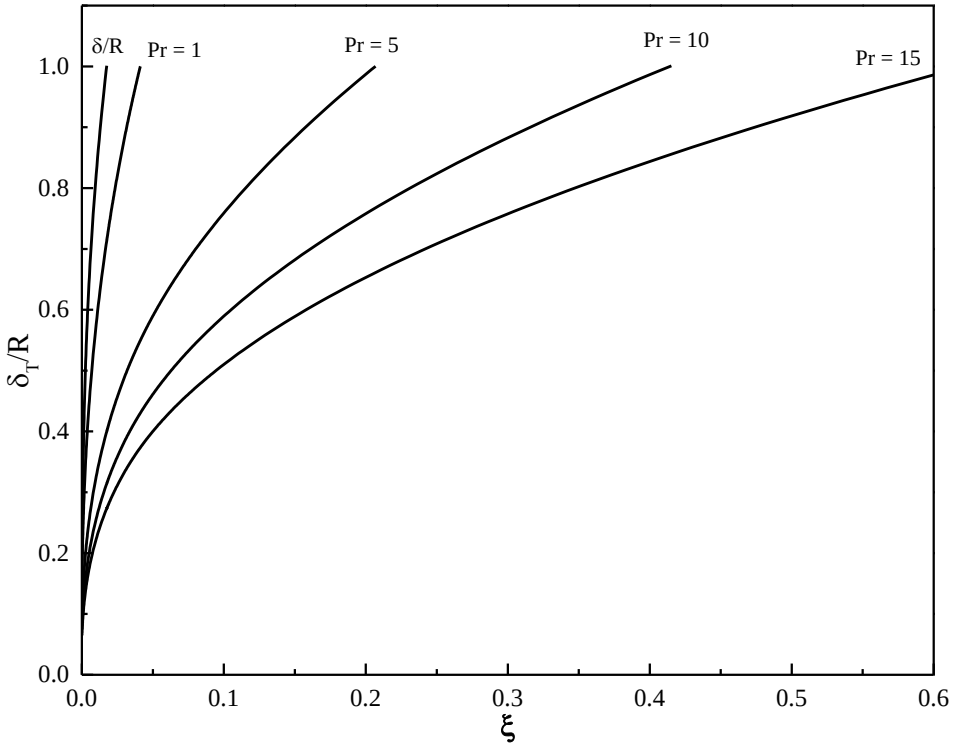

Figure 4-3. Hydrodynamic and Thermal Boundary Layer Thicknesses for Different Prandtl Numbers at *n = 1.4*

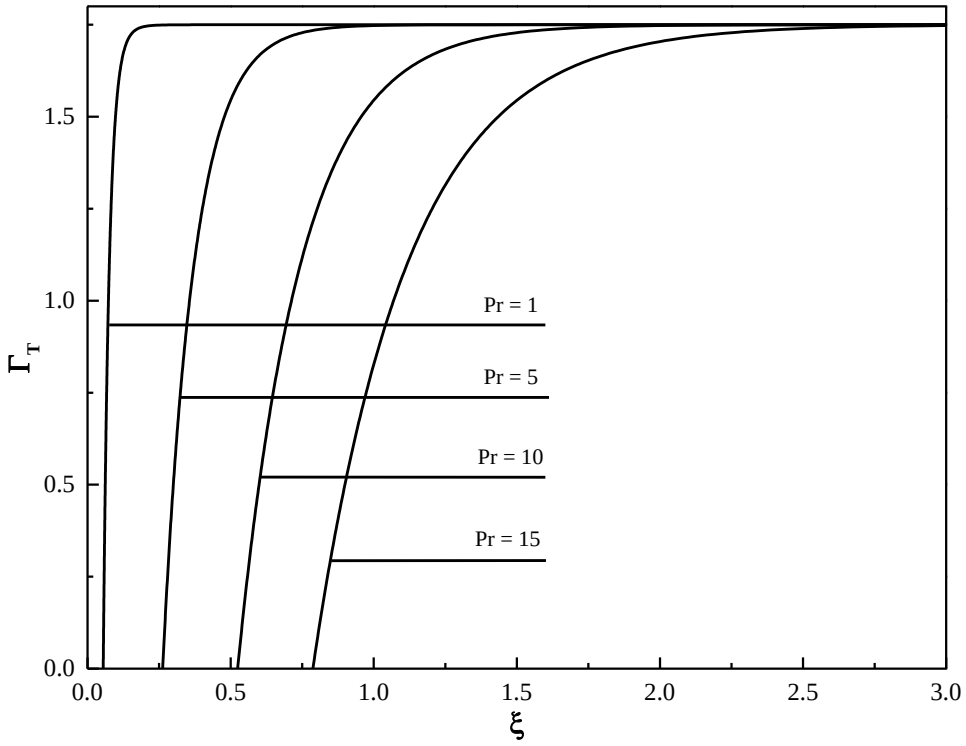

Figure 4-4. Thermal Shape Factor for Different Prandtl Numbers at *n = 0.6*

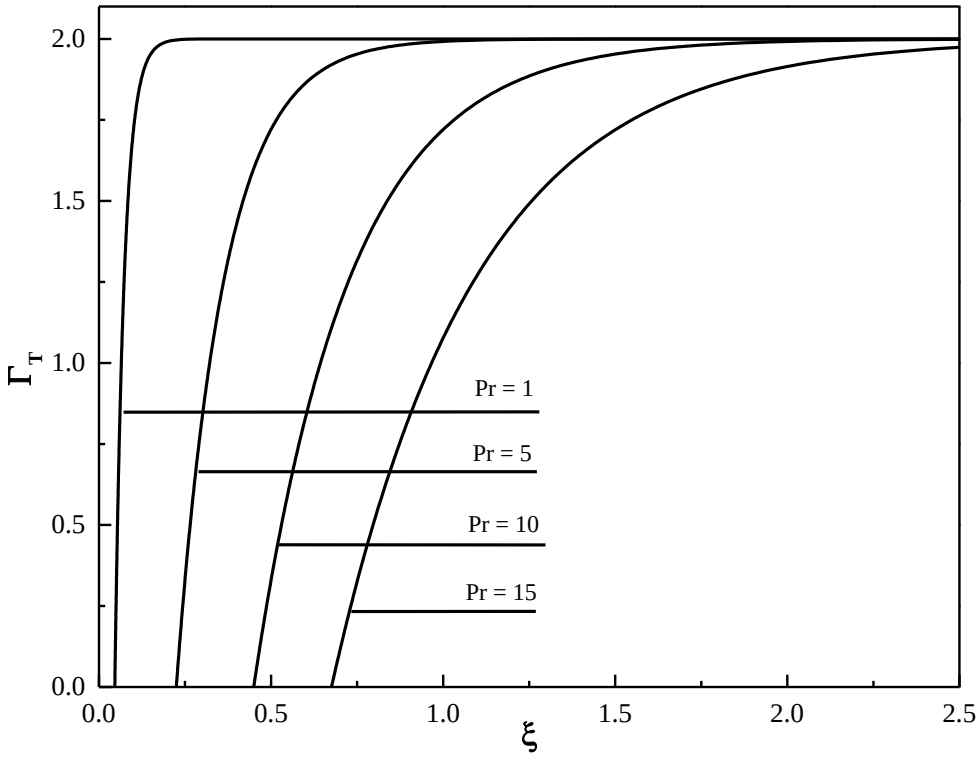

Figure 4-5. Thermal Shape Factor for Different Prandtl Numbers at *n = 1*

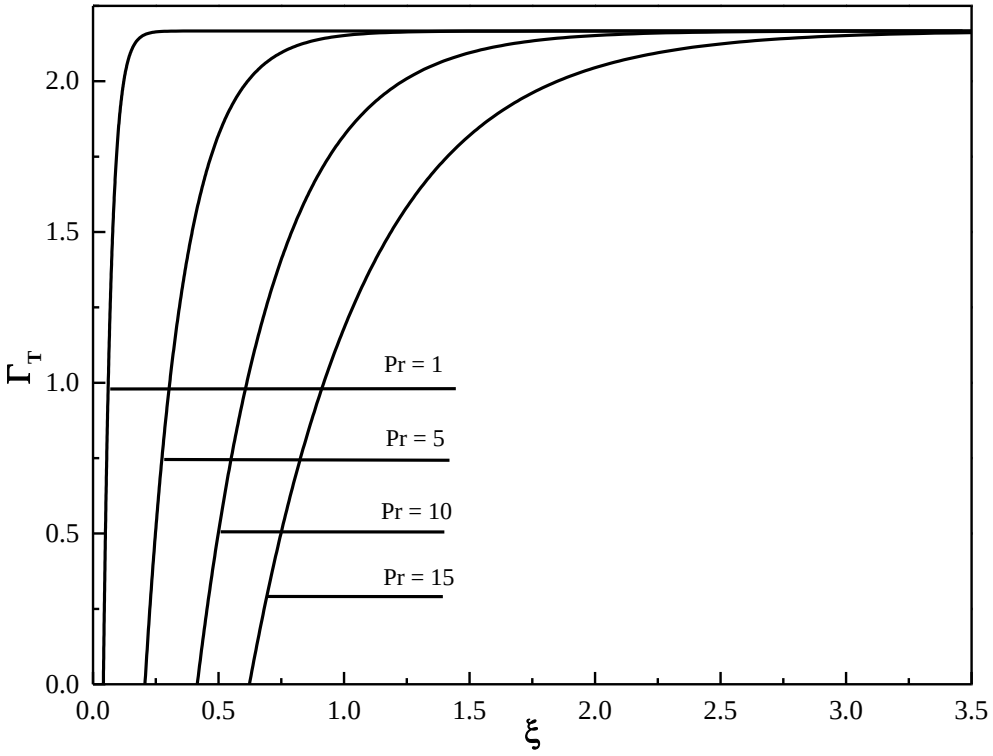

Figure 4-6. Thermal Shape Factor for Different Prandtl Numbers at *n = 1.4*

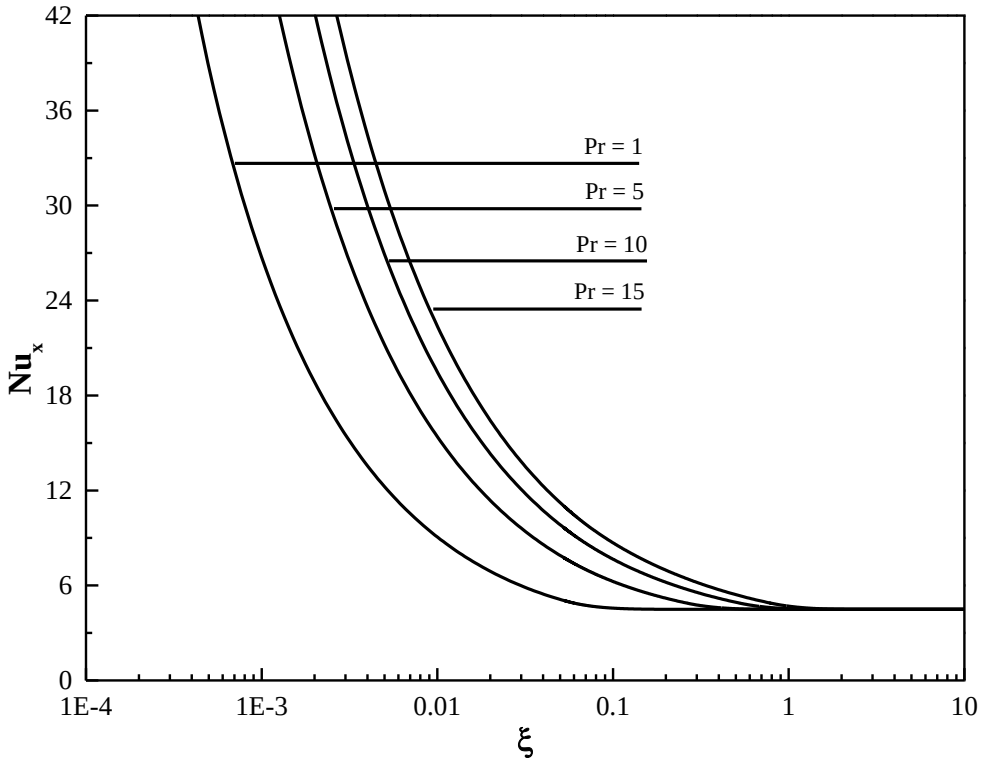

Figure 4-7. Local Nusselt Number for Different Prandtl Numbers at *n = 0.6*

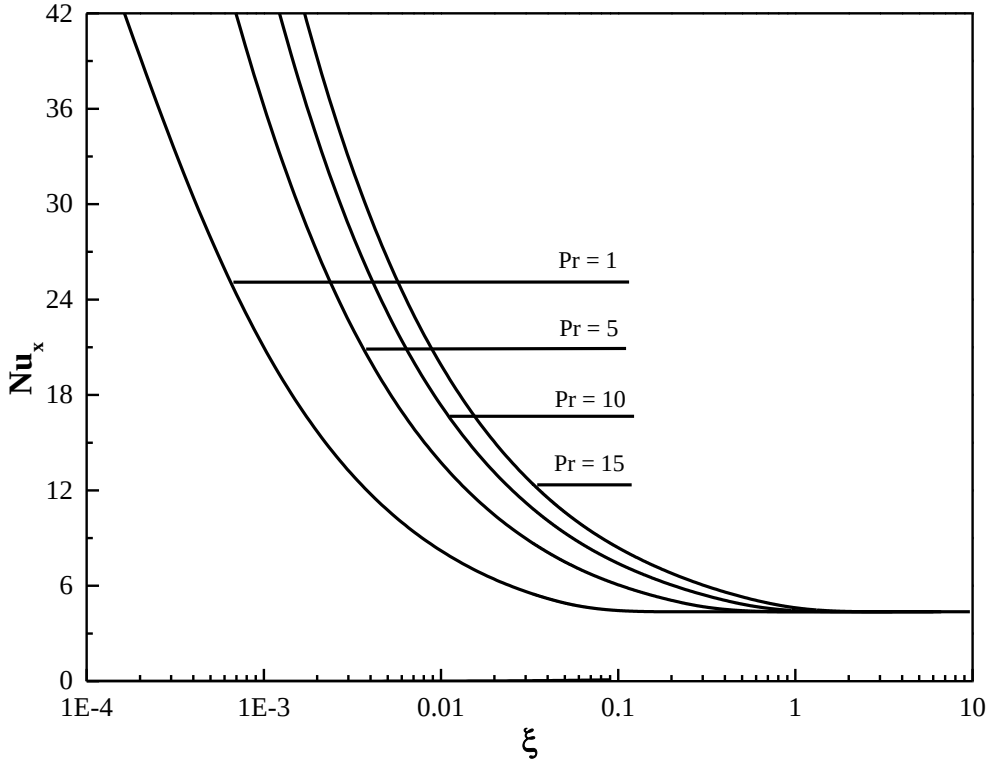

Figure 4-8. Local Nusselt Number for Different Prandtl Numbers at *n = 1*

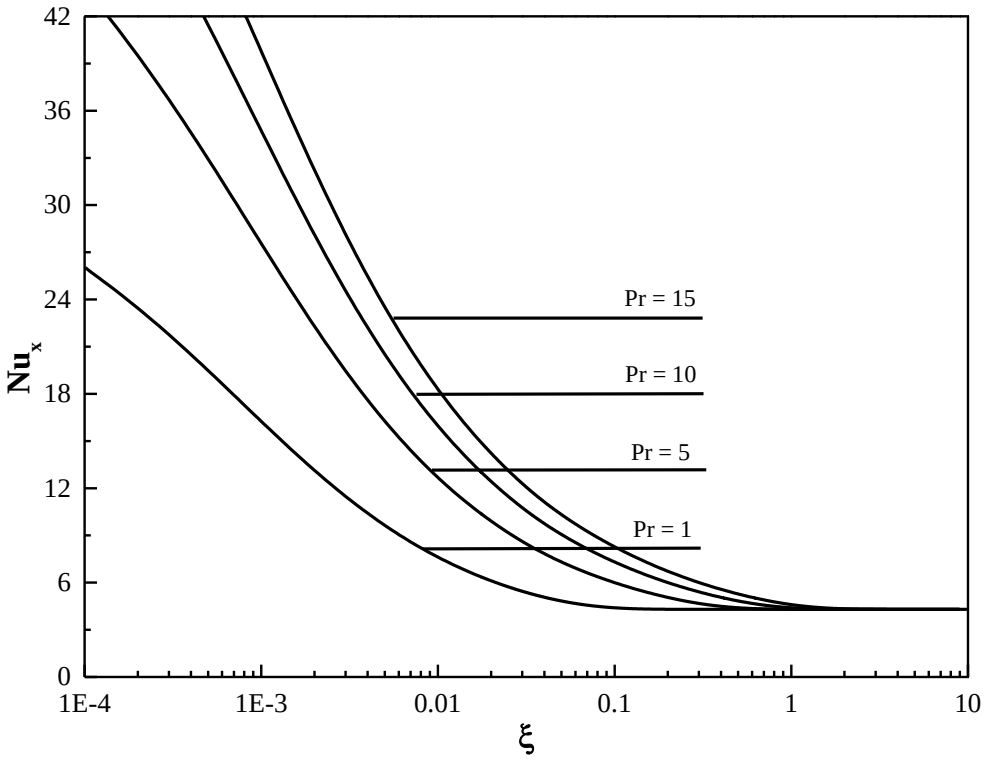

Figure 4-9. Local Nusselt Number for Different Prandtl Numbers at *n = 1.4*

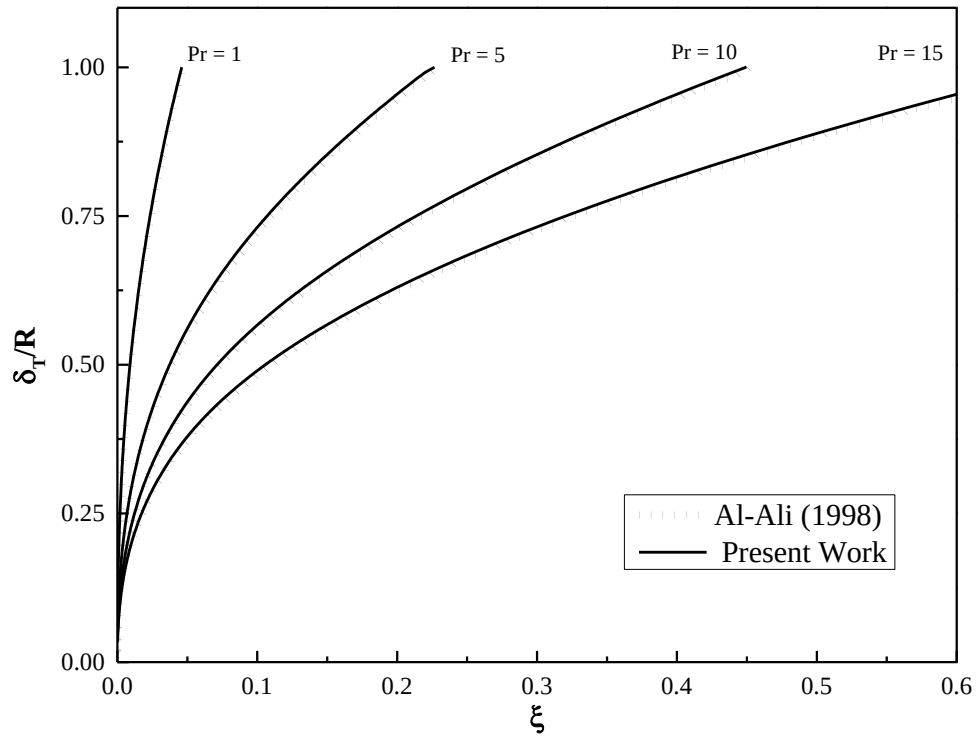

Figure 4-10. Comparison of Thermal Profiles for Different Prandtl Numbers by [35] at *n = 1*

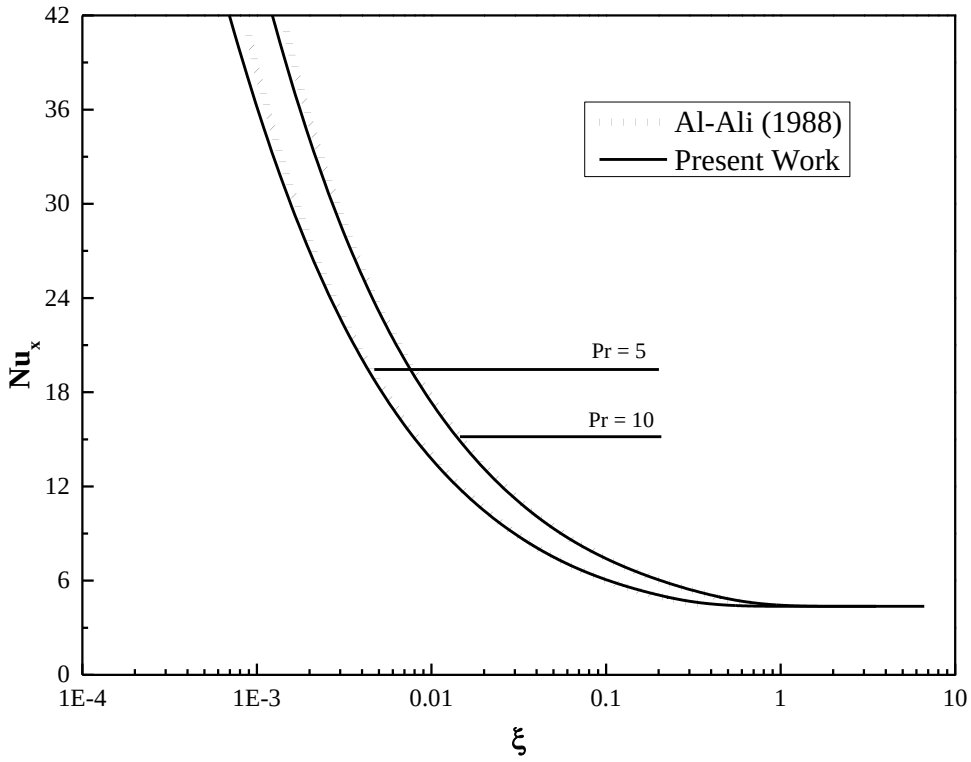

Figure 4-11. Comparison of the Local Nusselt Number for Different Prandtl Numbers by [35] at *n = 1*

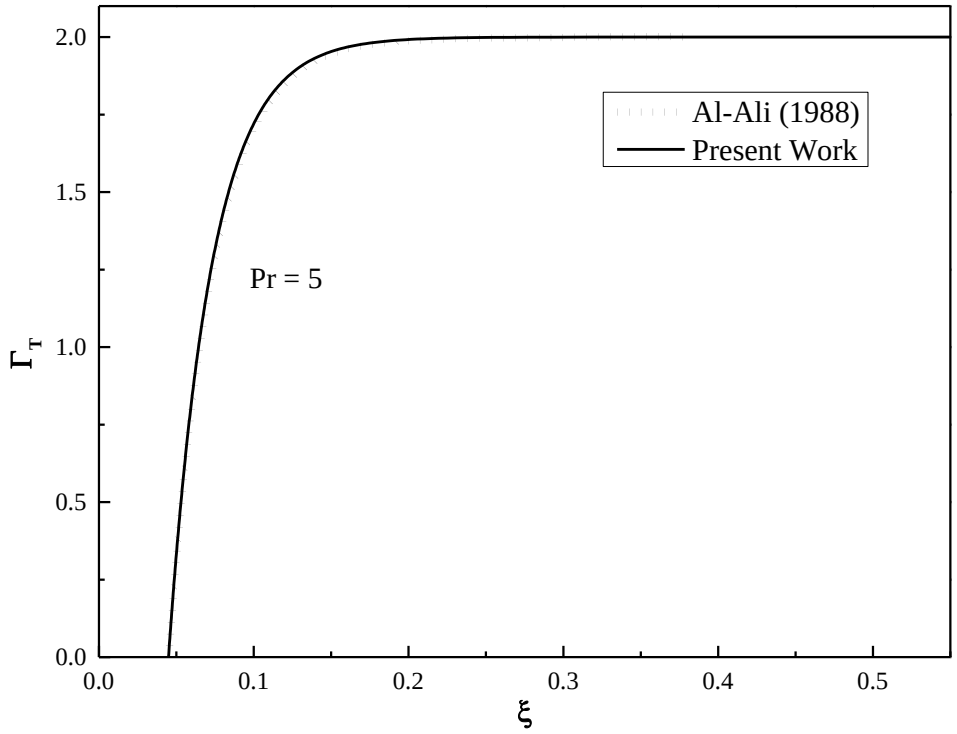

Figure 4-12. Comparison of Thermal Shape Factor by [35] at *n = 1*

Table 4.1: Thermal inlet region results for a pipe under constant heat flux ($n = 0.6$)

Pr=1			Pr=5			Pr=10			Pr=15		
ξ	$\bar{\delta}_T$	Nu	ξ	$\bar{\delta}_T$	Nu	ξ	$\bar{\delta}_T$	Nu	ξ	$\bar{\delta}_T$	Nu
0.002	0.22	18.04	0.002	0.12	31.73	0.002	0.09	40.35	0.002	0.08	46.40
0.014	0.53	7.94	0.014	0.29	13.32	0.014	0.23	16.83	0.014	0.20	19.32
0.053	0.98	5.05	0.053	0.52	7.74	0.053	0.41	9.64	0.053	0.35	11.00
0.054	0.99	5.02	0.054	0.53	7.68	0.054	0.41	9.56	0.054	0.35	10.91
0.055	1.00	5.00	0.055	0.53	7.63	0.055	0.41	9.49	0.055	0.36	10.83
			0.069	0.59	7.04	0.069	0.45	8.71	0.069	0.39	9.93
			0.100	0.68	6.24	0.100	0.53	7.65	0.100	0.45	8.68
			0.146	0.79	5.62	0.146	0.61	6.80	0.146	0.52	7.68
			0.189	0.87	5.26	0.189	0.67	6.30	0.189	0.57	7.08
			0.262	1.00	4.89	0.263	0.76	5.76	0.263	0.65	6.43
						0.288	0.79	5.62	0.288	0.67	6.26
						0.525	1.00	4.89	0.549	0.86	5.30
									0.787	1.00	4.89

Table 4.2: Thermally filled region results for a pipe under constant heat flux ($n = 0.6$)

Pr=1			Pr=5			Pr=10			Pr=15		
ξ	Γ_T	Nu	ξ	Γ_T	Nu	ξ	Γ_T	Nu	ξ	Γ_T	Nu
0.056	0.11	4.96	0.276	0.21	4.84	0.553	0.21	4.84	0.829	0.21	4.84
0.061	0.44	4.87	0.293	0.42	4.79	0.586	0.42	4.79	0.879	0.42	4.79
0.068	0.82	4.76	0.311	0.62	4.74	0.621	0.62	4.74	0.932	0.62	4.74
0.071	0.91	4.74	0.375	1.12	4.63	0.750	1.12	4.63	1.125	1.12	4.63
0.076	1.09	4.69	0.507	1.56	4.53	1.013	1.56	4.53	1.520	1.56	4.53
0.079	1.18	4.67	0.557	1.63	4.52	1.114	1.63	4.52	1.671	1.63	4.52
0.082	1.26	4.64	0.714	1.72	4.50	1.428	1.72	4.50	2.142	1.72	4.50
0.355	1.75	4.49	0.874	1.74	4.49	1.748	1.74	4.49	2.621	1.74	4.49
0.727	1.75	4.49	2.308	1.75	4.49	4.731	1.75	4.49	6.935	1.75	4.49

Table 4.3: Thermal inlet region results for a pipe under constant heat flux ($n = 1$)

Pr=1			Pr=5			Pr=10			Pr=15		
ξ	$\bar{\delta}_T$	Nu	ξ	$\bar{\delta}_T$	Nu	ξ	$\bar{\delta}_T$	Nu	ξ	$\bar{\delta}_T$	Nu
0.000	0.13	31.13	0.000	0.07	53.42	0.000	0.06	67.44	0.000	0.05	77.29
0.002	0.26	15.63	0.002	0.15	26.87	0.002	0.12	33.98	0.002	0.10	39.00
0.008	0.47	9.04	0.008	0.26	15.26	0.008	0.21	19.26	0.008	0.18	22.10
0.035	0.89	5.39	0.035	0.49	8.49	0.035	0.38	10.60	0.035	0.33	12.12
0.041	0.96	5.15	0.041	0.52	8.01	0.041	0.41	9.98	0.041	0.35	11.39
0.046	1.00	5.01	0.046	0.54	7.72	0.046	0.42	9.60	0.046	0.37	10.95
			0.060	0.60	7.07	0.060	0.47	8.75	0.060	0.41	9.96
			0.098	0.73	6.09	0.098	0.56	7.45	0.098	0.49	8.44
			0.117	0.78	5.81	0.117	0.60	7.06	0.117	0.52	7.98
			0.225	1.00	4.96	0.227	0.77	5.85	0.227	0.66	6.54
						0.255	0.80	5.67	0.257	0.69	6.32
						0.450	1.00	4.95	0.477	0.87	5.37
									0.613	0.96	5.06
									0.676	1.00	4.95

Table 4.4: Thermally filled region results for a pipe under constant heat flux ($n = 1$)

Pr=1			Pr=5			Pr=10			Pr=15		
ξ	Γ_T	Nu	ξ	Γ_T	Nu	ξ	Γ_T	Nu	ξ	Γ_T	Nu
0.049	0.19	4.94	0.247	0.30	4.86	0.495	0.30	4.86	0.744	0.30	4.86
0.052	0.39	4.87	0.274	0.60	4.76	0.549	0.60	4.76	0.824	0.60	4.76
0.055	0.58	4.81	0.304	0.86	4.68	0.608	0.86	4.68	0.913	0.86	4.68
0.063	0.94	4.69	0.374	1.31	4.55	0.749	1.31	4.55	1.125	1.31	4.55
0.068	1.11	4.63	0.418	1.50	4.50	0.836	1.50	4.50	1.255	1.50	4.50
0.074	1.27	4.58	0.469	1.65	4.46	0.939	1.65	4.46	1.409	1.65	4.46
0.080	1.42	4.53	0.532	1.78	4.42	1.064	1.78	4.42	1.597	1.78	4.42
0.087	1.55	4.49	0.613	1.88	4.40	1.227	1.88	4.40	1.841	1.88	4.40
0.096	1.68	4.46	0.728	1.95	4.38	1.456	1.95	4.38	2.185	1.95	4.38
0.107	1.78	4.43	0.851	1.98	4.37	1.701	1.98	4.37	2.551	1.98	4.37
0.122	1.87	4.40	0.926	1.99	4.37	1.851	1.99	4.37	2.775	1.99	4.37
0.143	1.94	4.38	1.155	2.00	4.36	2.309	2.00	4.36	3.461	2.00	4.36
0.307	2.00	4.36	2.370	2.00	4.36	4.638	2.00	4.36	6.838	2.00	4.36
0.610	2.00	4.36	3.528	2.00	4.36	6.648	2.00	4.36	9.661	2.00	4.36

Table 4.5: Thermal inlet region results for a pipe under constant heat flux ($n = 1.4$)

)Pr=1			Pr=5			Pr=10			Pr=15		
ξ	$\bar{\delta}_T$	Nu	ξ	$\bar{\delta}_T$	Nu	ξ	$\bar{\delta}_T$	Nu	ξ	$\bar{\delta}_T$	Nu
0.000	0.18	22.89	0.000	0.11	38.56	0.000	0.08	48.48	0.000	0.07	55.46
0.002	0.30	13.80	0.002	0.17	23.42	0.002	0.14	29.54	0.002	0.12	33.86
0.009	0.56	7.83	0.009	0.31	13.07	0.009	0.25	16.46	0.009	0.22	18.86
0.018	0.72	6.29	0.018	0.41	10.24	0.018	0.32	12.85	0.018	0.28	14.71
0.030	0.89	5.44	0.030	0.49	8.59	0.030	0.38	10.73	0.030	0.33	12.26
0.039	0.98	5.10	0.039	0.54	7.89	0.039	0.42	9.82	0.039	0.37	11.21
0.041	1.00	5.04	0.041	0.55	7.77	0.041	0.43	9.66	0.041	0.37	11.02
			0.178	0.94	5.19	0.186	0.74	6.12	0.192	0.64	6.81
			0.207	1.00	5.02	0.222	0.79	5.84	0.232	0.69	6.45
						0.415	1.00	5.02	0.455	0.89	5.40
									0.537	0.94	5.19
									0.623	1.00	5.02

Table 4.6: Thermally filled region results for a pipe under constant heat flux ($n = 1.4$)

Pr=1			Pr=5			Pr=10			Pr=15		
ξ	Γ_T	Nu	ξ	Γ_T	Nu	ξ	Γ_T	Nu	ξ	Γ_T	Nu
0.044	0.16	4.97	0.226	0.25	4.93	0.454	0.25	4.93	0.681	0.25	4.93
0.047	0.35	4.90	0.249	0.50	4.84	0.499	0.50	4.84	0.749	0.50	4.84
0.064	1.12	4.62	0.360	1.34	4.55	0.722	1.34	4.55	1.083	1.34	4.55
0.070	1.31	4.56	0.396	1.50	4.50	0.793	1.50	4.50	1.189	1.50	4.50
0.077	1.47	4.51	0.435	1.65	4.45	0.872	1.65	4.45	1.308	1.65	4.45
0.085	1.62	4.46	0.481	1.78	4.42	0.962	1.78	4.42	1.444	1.78	4.42
0.094	1.75	4.42	0.533	1.89	4.38	1.068	1.89	4.38	1.602	1.89	4.38
0.104	1.87	4.39	0.596	1.98	4.36	1.194	1.98	4.36	1.791	1.98	4.36
0.116	1.96	4.36	0.675	2.05	4.33	1.351	2.05	4.33	2.027	2.05	4.33
0.131	2.04	4.34	0.780	2.11	4.32	1.561	2.11	4.32	2.341	2.11	4.32
0.151	2.10	4.32	0.937	2.14	4.31	1.874	2.14	4.31	2.810	2.14	4.31
0.179	2.14	4.31	1.255	2.16	4.30	2.510	2.16	4.30	3.761	2.16	4.30
0.7205	2.17	4.30	3.4639	2.17	4.30	7.4130	2.17	4.30	12.2323	2.17	4.30

Table 4.7: Thermal entrance length based on the Nusselt number criterion for a pipe under constant wall temperature ($n = 0.6$)

Pr	$\xi_{in,T}$	$(\xi/\mathrm{Pr})_{in,T}$	ξ_T	$(\xi/\mathrm{Pr})_T$	$\xi_T - \xi_{in,T}$	$\frac{\xi_{in,T}}{\xi_T}$	$\frac{\xi_T - \xi_{in,T}}{\xi_T}$
1	0.0548	0.0548	0.0731	0.0731	0.0183	0.75	0.25
5	0.2624	0.0525	0.3222	0.0644	0.0598	0.81	0.19
10	0.5245	0.0525	0.6416	0.0616	0.1171	0.82	0.18
15	0.7872	0.0525	0.9666	0.0644	0.1794	0.81	0.19

Table 4.8: Thermal entrance length based on the Nusselt number criterion for a pipe under constant wall temperature ($n = 1$)

Pr	$\xi_{in,T}$	$(\xi/\mathrm{Pr})_{in,T}$	ξ_T	$(\xi/\mathrm{Pr})_T$	$\xi_T - \xi_{in,T}$	$\frac{\xi_{in,T}}{\xi_T}$	$\frac{\xi_T - \xi_{in,T}}{\xi_T}$
1	0.0460	0.0460	0.0736	0.0736	0.0276	0.62	0.38
5	0.2246	0.0449	0.3532	0.0706	0.1286	0.64	0.36
10	0.4496	0.0449	0.7066	0.0706	0.2570	0.64	0.36
15	0.6756	0.0450	1.0609	0.0707	0.3853	0.64	0.36

Table 4.9: Thermal entrance length based on the Nusselt number criterion for a pipe under constant wall temperature ($n = 1.4$)

Pr	$\xi_{in,T}$	$(\xi/\mathrm{Pr})_{in,T}$	ξ_T	$(\xi/\mathrm{Pr})_T$	$\xi_T - \xi_{in,T}$	$\frac{\xi_{in,T}}{\xi_T}$	$\frac{\xi_T - \xi_{in,T}}{\xi_T}$
1	0.0411	0.0411	0.0763	0.0763	0.0352	0.54	0.46
5	0.2068	0.0414	0.3831	0.0766	0.1763	0.54	0.46
10	0.4152	0.0415	0.7676	0.0768	0.3524	0.54	0.46
15	0.6232	0.0415	1.1515	0.0768	0.5283	0.54	0.46

Chapter 5. Conclusion and Recommendations

5.1. Summary

Chapter 2 highlighted the background and existing literature on the topic. It states the techniques used to solve this problem by different investigators. Chapter 3 outlined the extension of Mohanty and Asthana's [6] approach to solve the hydrodynamic and thermal boundary layer thicknesses simultaneously for power-law fluids. The procedure and the numerical solution of the resulting equations is presented in Chapter 4. Furthermore, graphs and tables for selected results are plotted and compared with results from the literature.

5.2. Conclusion

The solution of the simultaneously developing power-law fluid flow and heat transfer for power-law fluids was addressed using the inlet-filled region concept along with the von Kármán momentum integral analytical method to solve the momentum and energy equations using the hydrodynamic entrance region model developed in [5] for power-law fluids and extending the heat transfer model in [35,36] for the Newtonian fluid flow case. The analysis provides the local Nusselt number and the thermal entrance length for various values power law indices n and different Prandtl numbers between 1 to 15. The thesis work provides the basis for the determination of heat transfer coefficients in heat exchangers. The thermal boundary layer thickness and local Nusselt number profiles for $n = 1$ and $\mathrm{Pr} = 5$ are in close agreement with the numerical results given in [30].

5.3. Future work

Experimental work for $n < 1$ and $n > 1$ at $Pr > 1$ could be conducted to compare the present results for the thermal boundary layer thickness profile, the local Nusselt number profile, and the thermal entrance region length with experimental data. In addition, viscous dissipation effects could be included.

References

[1] S. D. Joshi, “Heat transfer in in-tube flow of non-Newtonian fluids,” PhD Thesis, Iowa State University, July 1978.

[2] W. Fliigge, “Viscoelasticity,” *Blaisdell Publ. Comp., London*, pp. 1069–1084, 1967.

[3] G. F. Cochrane, “A numerical solution for heat transfer to non-Newtonian fluids with temperature-dependent viscosity for arbitrary conditions of heat flux and surface temperature,” PhD Thesis, Oregon State University, June 1969.

[4] W. L. Wilkinson, *Non-Newtonian fluids: fluid mechanics, mixing and heat transfer*, vol. 1. Pergamon, 1960.

[5] R. Chebbi, “Laminar flow of power-law fluids in the entrance region of a pipe,” *Chem. Eng. Sci.*, vol. 57, no. 21, pp. 4435–4443, 2002, doi: https://doi.org/10.1016/S0009-2509(02)00422-0

[6] A. K. Mohanty and S. B. L. Asthana, “Laminar flow in the entrance region of a smooth pipe,” *J. Fluid Mech.*, vol. 90, no. 3, pp. 433–447, 1979.

[7] R. Chebbi, H. H. Al-Ali, and M. Sami Selim, “Simultaneously developing laminar flow and heat transfer in the entrance region of a circular tube with constant wall temperature,” *Chem. Eng. Commun.*, vol. 160, no. 1, pp. 59–70, 1997.

[8] S. Ishizawa, “The Axi-Symmetric Laminar Flow in an Arbitrarily Shaped Narrow Gap:(2nd Report, Theoretical Analysis for the Downstream Region),” *Bull. JSME*, vol. 9, no. 33, pp. 86–103, 1966.

[9] von L. Graetz, “Über die wärmeleitungsfähigkeit von flüssigkeiten,” *Ann. Phys.*, vol. 261, no. 7, pp. 337–357, 1885.

[10] W. Nusselt, *Die abhängigkeit der wärmeübergangszahl von der rohrlänge*. VDI, 1910.

[11] A. Lévêque, “Les lois de la transmission de chaleur par convection...” Dunod, Paris Press, 1928.

[12] S. D. Joshi, “Heat transfer in in-tube flow of non-Newtonian fluids,” PhD Thesis, Iowa State University, July 1978.

[13] Y.-P. Shih and J.-D. Tsou, “Extended leveque solutions for heat transfer to power law fluids in laminar flow in a pipe,” *Chem. Eng. J.*, vol. 15, no. 1, pp. 55–62, 1978.

[14] A. Belhocine and W. Z. W. Omar, “Exact Graetz problem solution by using hypergeometric function,” *Int J Heat Technol*, vol. 35, no. 2, pp. 347–353, 2017.

[15] J. R. Sellars, M. Tribus, and J. Klein, “Heat transfer to laminar flow in a round tube or flat conduit: the Graetz probem extended,” University of Michigan Library, 1954.

[16] A. Silva Telles, E. M. Queiroz, and G. E. Filho, “Solutions of the extended Graetz problem,” *Int. J. Heat Mass Transf.*, vol. 44, no. 2, pp. 471–483, 2001, doi: https://doi.org/10.1016/S0017-9310(00)00107-1

[17] C.-T. Liou and F.-S. Wang, “Solutions to the extended Graetz problem for a power-model fluid with viscous dissipation and different entrance boundary conditions,” *Numer. heat Transf.*, vol. 17, no. 1, pp. 91–108, 1990.

[18] R. Siegel, E. M. Sparrow, and T. M. Hallman, “Steady laminar heat transfer in a circular tube with prescribed wall heat flux,” *Appl. Sci. Res. Sect. A*, vol. 7, no. 5, pp. 386–392, 1958.

[19] W. M. Kays, “Numerical solution for laminar-flow heat transfer in circular tube,” *Trans. ASME*, vol. 77, pp. 1265–1274, 1955.

[20] C.-L. Hwang, “A finite difference analysis of magnetohydrodynamic flow with forced convection heat transfer in the entrance region of a flat rectangular duct”. PhD Thesis, Kansas State University, 1962.

[21] C.-L. Hwang and L.-T. Fan, “A finite difference analysis of laminar magnetohydrodynamic flow in the entrance region of a flat rectangular duct,” *Appl. Sci. Res. Sect. B*, vol. 10, no. 3–4, p. 329, 1963.

[22] C.-L. Hwang and L.-T. Fan, “Finite difference analysis of forced-convection heat transfer in entrance region of a flat rectangular duct,” *Appl. Sci. Res. Sect. A*, vol. 13, no. 1, pp. 401–422, 1964.

[23] B. C. Lyche and R. B. Bird, “The Graetz-Nusselt problem for a power-law nonnewtonian fluid,” *Chem. Eng. Sci.*, vol. 6, no. 1, pp. 35–41, 1956, doi: https://doi.org/10.1016/0009-2509(56)80008-0

[24] J. Yau and C. Tien, “Simultaneous development of velocity and temperature profiles for laminar flow of a non-Newtonian fluid in the entrance region of flat ducts,” *Can. J. Chem. Eng.*, vol. 41, no. 4, pp. 139–145, 1963.

[25] A. A. McKillop, “Heat transfer for laminar flow of non-Newtonian fluids in entrance region of a tube,” *Int. J. Heat Mass Transf.*, vol. 7, no. 8, pp. 853–862, 1964.

[26] Atinkson and G. S., *Modern Developments in Fluid Dynamics, Vol. 1*. Oxford University Press, 1938.

[27] R. B. Bird, “Zur Theorie des Wärmeübergangs an nicht-Newtonsche Flüssigkeiten bei laminarer Rohrströmung,” *Chemie Ing. Tech.*, vol. 31, no. 9, pp. 569–572, 1959.

[28] B. T. F. Chung and Z. J. Zhang, “Heat transfer from thermally developing flow of non-Newtonian fluids in rectangular ducts,” *WIT Trans. Eng. Sci.*, vol. 5, no. 10, pp. 183-190, 1970.

[29] R. M. Cotta and M. N. Özişik, “Laminar forced convection to non-Newtonian fluids in ducts with prescribed wall heat flux,” *Int. Commun. heat mass Transf.*, vol. 13, no. 3, pp. 325–334, 1986.

[30] C. L. Chaves, J. N. N. Quaresma, E. N. Macedo, L. M. Pereira, and J. A. Lima, “Forced convection heat transfer to power-law non-Newtonian fluids inside triangular ducts,” *Heat Transf. Eng.*, vol. 25, no. 7, pp. 23–33, 2004.

[31] J. N. N. Quaresma and E. N. Macêdo, “Integral transform solution for the forced convection of Herschel-Bulkley fluids in circular tubes and parallel-plates ducts,” *Brazilian J. Chem. Eng.*, vol. 15, 1998.

[32] J. N. N. Quaresma and J. A. Lima, “Thermally developing turbulent flow of pseudoplastic fluids within circular tubes,” *Int. Commun. heat mass Transf.*, vol. 25, no. 8, pp. 1105–1114, 1998.

[33] R. N. O. Magno, E. N. Macedo, and J. N. N. Quaresma, “Solutions for the internal boundary layer equations in simultaneously developing flow of powerlaw fluids within parallel plates channels,” *Chem. Eng. J.*, vol. 87, no. 3, pp. 339– 350, 2002.

[34] D. Crespí-Llorens and N. Galanis, “Laminar forced convection of power-law fluids in the entrance region of parallel plates ducts,” *Int. J. Heat Mass Transf.*, vol. 115, pp. 991–1003, 2017.

[35] H. H. Al-Ali, “Simultaneously developing laminar flow and heat transfer in the entrance region of flat and circular conduits.,” PhD Thesis, Colorado School of Mines, September 1988.

[36] H. H. Al-Ali and M. Sami Selim, “Analysis of laminar flow forced convection heat transfer with uniform heating in the entrance region of a circular tube,” *Can. J. Chem. Eng.*, vol. 70, no. 6, pp. 1101–1107, 1992.

[37] H. I. Andersson, K. H. Bech, and B. S. Dandapat, “Magnetohydrodynamic flow of a power-law fluid over a stretching sheet,” *Int. J. Non. Linear. Mech.*, vol. 27, no. 6, pp. 929–936, 1992, doi: https://doi.org/10.1016/0020-7462(92)90045-9

[38] R. Bird, W. Stewart, and E. Lightfoot, *Transport Phenomena* 2nd edition john wiley and sons, Wiley Publisher, New York, 2002.

Vita

Muhammad Faheem Hassan born and raised in Rawalpindi, Pakistan. He received his B.Sc. degree in Chemical Engineering from MNS-University of Engineering and Technology, Multan, Pakistan in 2016.

In September 2019, he joined the Chemical Engineering master's program in the American University of Sharjah as a graduate teaching assistant. He developed a heat transfer model to solve the combined entry length problem for power-law fluid flow in a pipe subjected to constant heat flux at the wall. During his studies at AUS, he published and presented his research work in areas including Ionic Liquids, Corrosion Inhibition, Wastewater Treatment, and Membrane Material Synthesis.